



HAL
open science

Waterpixels

Vaïa Machairas, Matthieu Faessel, David Cárdenas-Peña, Théodore Chabardes, Thomas Walter, Etienne Decencière

► **To cite this version:**

Vaïa Machairas, Matthieu Faessel, David Cárdenas-Peña, Théodore Chabardes, Thomas Walter, et al. Waterpixels. IEEE Transactions on Image Processing, 2015, 24 (11), pp.3707 - 3716. 10.1109/TIP.2015.2451011 . hal-01212760

HAL Id: hal-01212760

<https://hal.science/hal-01212760v1>

Submitted on 7 Oct 2015

HAL is a multi-disciplinary open access archive for the deposit and dissemination of scientific research documents, whether they are published or not. The documents may come from teaching and research institutions in France or abroad, or from public or private research centers.

L'archive ouverte pluridisciplinaire **HAL**, est destinée au dépôt et à la diffusion de documents scientifiques de niveau recherche, publiés ou non, émanant des établissements d'enseignement et de recherche français ou étrangers, des laboratoires publics ou privés.

Waterpixels

Vaia Machairas, Matthieu Faessel, David Cárdenas-Peña, Théodore Chabardes,
Thomas Walter, and Etienne Decencière

1 **Abstract**—Many approaches for image segmentation rely on a
2 first low-level segmentation step, where an image is partitioned
3 into homogeneous regions with enforced regularity and adherence
4 to object boundaries. Methods to generate these superpixels have
5 gained substantial interest in the last few years, but only a few
6 have made it into applications in practice, in particular because
7 the requirements on the processing time are essential but are not
8 met by most of them. Here, we propose waterpixels as a general
9 strategy for generating superpixels which relies on the marker
10 controlled watershed transformation. We introduce a spatially
11 regularized gradient to achieve a tunable tradeoff between the
12 superpixel regularity and the adherence to object boundaries.
13 The complexity of the resulting methods is linear with respect
14 to the number of image pixels. We quantitatively evaluate our
15 approach on the Berkeley segmentation database and compare
16 it against the state-of-the-art.

17 **Index Terms**—Superpixels, watershed, segmentation.

I. INTRODUCTION

18
19 **SUPERPIXELS** (SP) are regions resulting from
20 a low-level segmentation of an image and are typically
21 used as primitives for further analysis such as detection,
22 segmentation, and classification of objects (see Figure 1
23 for an illustration). The underlying idea is that this first
24 low-level partition alleviates the computational complexity of
25 the following processing steps and improves their robustness,
26 as not single pixel values but pixel set features can be used.

27 Superpixels should have the following properties:

28 1) **homogeneity**: pixels of a given SP should present
29 similar colors or gray levels;



Fig. 1. Superpixels illustration. The original image comes from the Berkeley segmentation database. (a) Original image. (b) Waterpixels.

- 2) **connected partition**: each SP is made of a single
connected component and the SPs constitute a partition
of the image;
- 3) **adherence to object boundaries**: object boundaries
should be included in SP boundaries;
- 4) **regularity**: SPs should form a regular pattern on the
image. This property is often desirable as it makes the
SP more convenient to use for subsequent analysis steps.

The requirements on regularity and boundary adherence
are to a certain extent oppositional, and a good solution
typically aims at finding a compromise between these two
requirements.

In addition to these requirements on superpixel quality,
computational efficiency is an absolutely essential aspect, as
the partition into superpixels is typically only the first step of
an often complex and potentially time consuming workflow.
Methods of linear complexity are consequently of particular
interest.

We therefore hypothesized that the Watershed transforma-
tion [1], [2] should be an interesting candidate for superpixel
generation, as it has been shown to achieve state-of-the-art
performance in many segmentation problems, it is
non-parametric, and there exist linear-complexity algorithms
to compute it, as well as efficient implementations [3], [4].
The only often cited drawback, oversegmentation, does not
seem to be problematic for superpixel generation, as long as
we can control the degree of oversegmentation (number of
superpixels), and the regularity of the resulting partition.

Given these considerations, we propose a strategy for
applying the watershed transform to superpixel generation,
where we use a spatially regularized gradient to achieve a
tunable trade-off between superpixel regularity and adherence
to object boundaries. We quantitatively evaluate our method
on the Berkeley segmentation database and show that we
outperform the best linear-time state-of-the-art method: Simple
Linear Iterative Clustering (SLIC) [5]. We call the resulting
superpixels “waterpixels.”

Manuscript received December 18, 2014; revised April 17, 2015; accepted
June 15, 2015. The work of T. Walter was supported by the European
Community through the Seventh Framework Programme (FP7/2007-2013)
within the Systems Microscopy under Grant 258068. The associate editor
coordinating the review of this manuscript and approving it for publication
was Dr. Yonggang Shi.

V. Machairas, M. Faessel, T. Chabardes, and E. Decencière are with
MINES ParisTech, Paris 75006, France, also with PSL Research University,
Paris 75005, France, and also with the Center for Mathematical Morphology,
Fontainebleau 77305, France (e-mail: vaia.machairas@mines-paristech.fr;
matthieu.faessel@mines-paristech.fr; theodore.chabardes@mines-paristech.fr;
etienne.decenciere@mines-paristech.fr).

D. Cárdenas-Peña is with the Signal Processing and Recognition Group,
Universidad Nacional de Colombia, Manizales 170001-17, Colombia (e-mail:
dcardenas@unal.edu.co).

T. Walter is with MINES ParisTech, Paris 75006, France, also with PSL
Research University, Paris 75005, France, also with the Centre for Compu-
tational Biology, Fontainebleau 77305, France, also with the Institut Curie,
Paris 75248, France, and also with Inserm, Paris 75248, France (e-mail:
thomas.walter@mines-paristech.fr).

Color versions of one or more of the figures in this paper are available
online at <http://ieeexplore.ieee.org>.

Digital Object Identifier 10.1109/TIP.2015.2451011

TABLE I
 RECAP CHART OF EXISTING METHODS TO COMPUTE REGULAR
 SUPERPIXELS (n IS THE NUMBER OF PIXELS IN THE IMAGE; i IS
 THE NUMBER OF ITERATIONS REQUIRED; N THE NUMBER
 OF SUPERPIXELS). “WP” CORRESPONDS TO OUR
 METHOD, CALLED “WATERPIXELS”

Method	[11]	[12]	[13]	[5]	WP
Generation type (see section II-B)	1	2	1 (iterated)	2	1
Seed type (see section II-A)	A	C	C	C	B
Control on number of SPs	yes	yes	yes	no	yes
Control on regularity	no	yes	no	yes	yes
Post-processing free	no	no	no	no	yes
Complexity	$O(n)$	$O(in\sqrt{N})$	$O(in)$	$O(n)$	$O(n)$

This paper is an extended version of [6]. It proposes a more general approach (elaborating a whole family of waterpixels generation methods), with a more thorough validation and improved results with regard to the trade-off between boundary adherence and regularity, as well as computation time. Moreover, we have developed and made available a fast implementation of waterpixels.

II. RELATED WORK

Low-level segmentations have been used for a long time as first step towards segmentation [7], [8]. The term superpixel was coined much later [9], albeit in a more constrained framework. This approach has raised increasing interest since then. Various methods exist to compute SPs, most of them based on graphs [10], geometrical flows [11] or k-means [5]. We will focus on linear complexity methods generating regular SPs.

Methods for SP generation are all based on two steps: an initialization step where either seeds or a starting partition are defined and a (potentially iterative) assignment step, where each pixel is assigned to one superpixel, starting from the initialization. In the next section, we are going to review previously published approaches for SP generation with respect to these aspects and compare them regarding various performance criteria. We limit the presentation of existing methods to those with linear complexity.

A. Choosing the Seeds

In the first step, a set of seeds is chosen, which are typically spaced regularly over the image plane and which can be either regions or single pixels:

- Type A seeds are independent of the image content. These are typically the cells or the centers of a regular grid.
- Type B seeds depend on the content of the image (compromise between a regular cover of the image plane and an adaption to the contour).
- Type C seeds are initially image independent, then they are iteratively refined to take into account the image contents.

If the seed does not depend on the image, an iterative refinement is usually preferable, and therefore more time

is spent on the computation of the SP. Type B methods may spend more time on finding appropriate seeds, but can therefore afford not to iterate the SP generation.

B. Building Superpixels From Seeds

In the second step, the partition into superpixels is built from the seeds. Among the methods with linear complexity, there are two main strategies for this:

Shortest Path Methods (Type 1) [11], [13]: these methods are based on region growing: they start from a set of seeds (points or regions) and successively extend them by incorporating pixels in their neighborhood according to a usually image dependent cost function until every pixel of the image plane has been assigned to exactly one superpixel. This process may or may not be iterated.

Shortest Distance Methods (Type 2) [5], [12]: these are iterative procedures inspired by the field of unsupervised learning, where at each iteration step, seeds (such as centroids) are calculated from the previous partition and pixels are then re-assigned to the closest seed (like for example the k -means approach).

Even though methods inspired by general clustering methods (type 2) seem appealing at first sight, in particular when they globally optimize a cost function, this class of methods does not guarantee connectivity of the superpixels for arbitrary choices of the pixel-seed distance (see [5], [12]). For instance, the distance metric proposed in [5] (a combination of Euclidean and grey level distance), leads to non-connected superpixels, which is undesirable. To solve this issue, a post-processing step is necessary, consisting either in relabeling the image so that every connected component has its own label (see [12]), leading to a more irregular distribution of SP sizes and shapes, or in reassigning isolated regions to the closest and large enough Superpixel, as in [5], leading to non-optimality of the solution and an unpredictable number of superpixels. In addition, such postprocessing increases the computational cost and can turn out to be the most time-consuming step when the image contains numerous small objects/details compared to the size of the Superpixel.

On the contrary, methods based on region growing (type 1) inherently implement a “path-type” distance, where the distance between two pixels does not only depend on value and position of the pixels themselves, but on values and positions along the path connecting them. Type 1 methods imply connected superpixel regions, for which the number of superpixels is exactly the number of seeds.

C. Other Properties

It is generally accepted that a good superpixel-generation method should provide to the user total control over the number of resulting Superpixels. While this property is achieved by [11]–[14], some only reach approximatively this number because of post-processing (either by splitting too big superpixels, or removing small isolated superpixels as in [5]). Another parameter is the control on superpixels regularity in the trade-off between regularity and adherence to contours. Only [5] and [12] enable the user to weight the importance

of regularity compared to boundary adherence, so it can be adapted to the application.

As far as performance is concerned, one of the main criteria is undoubtedly the complexity that the method requires. Indeed, for Superpixels to be used as primitives for further analysis such as classification, their computation should neither take too long nor too much memory. This is the reason why we focus on linear complexity methods. Among them, SLIC appears to offer the best performance with regards to the trade-off between adherence to boundaries and regularity [5]. Moreover, since its recent inception, this method has become very popular in the computer vision community. We will therefore use it as reference for the quantitative evaluation of our method.

D. Superpixels and Watershed

In principle, the watershed transformation (see [15] for a review) is well suited for SP generation:

- 1) It gives a good adherence to object boundaries when computed on the image gradient.
- 2) It allows to control the number and spatial arrangement of the resulting regions through the choice of markers.
- 3) The connectivity of resulting regions is guaranteed and no postprocessing is required.
- 4) It offers linear complexity with the number of pixels in the image.

Indeed, it has been used to produce low-level segmentations in several applications, including computation intensive 3D applications [16], [17], in particular when shape regularity of the elementary regions was not required.

Previous publications claimed that the watershed transformation does not allow for the generation of spatially regular SP [5], [11]. Recently, we and others [6], [18] have shown that in principle the watershed transformation can be applied to SP generation.

Here, we introduce waterpixels, a family of methods based on the watershed transformation to compute superpixels.

III. WATERPIXELS

As most watershed-based segmentation methods, waterpixels are based on two steps: the definition of markers, from which the flooding starts, and the definition of a gradient (the image to be flooded). We propose to design these steps in such a way that regularity is encouraged.

A waterpixel-generation method is characterized by the following steps:

- 1) Computation of the gradient of the image;
- 2) Definition of regular cells on the image, centered on the vertices of a regular grid;
- 3) Selection of one marker per cell;
- 4) Spatial regularization of the gradient with the help of a distance function;
- 5) Application of the watershed transformation on the regularized gradient defined in step 4 from the markers defined in step 2.

These steps are illustrated in figure 2 and developed in the next paragraphs.

A. Gradient and Cells Definition

Let $f : D \rightarrow V$ be an image, where D is a rectangular subset of Z^2 , and V a set of values, typically $\{0, \dots, 255\}$ when f is a grey level image, or $\{0, \dots, 255\}^3$ for color images.

The first step consists in computing the gradient image g of the image f . The choice of the gradient operator depends on the image type, *e.g.* for grey level images we might choose a morphological gradient. This gradient will be used to choose the seeds (section III-B) and to build the regularised gradient (III-C).

For the definition of cells, we first choose a set of N points $\{o_i\}_{1 \leq i \leq N}$ in D , called *cell centers*, so that they are placed on the vertices of a regular grid (a square or hexagonal one for example). Given a distance d on D , we denote by σ the grid step, *i.e.* the distance between closest grid points.

A Voronoi tessellation allows to associate to each o_i a Voronoi cell. For each such cell, a homothety centered on o_i with factor ρ ($0 < \rho \leq 1$) leads to the computation of the final cell C_i . This last step allows for the creation of a margin between neighbouring cells, in order to avoid the selection of markers too close from each other.

B. Selection of the Markers

As each cell is meant to correspond to the generation of a unique waterpixel, our method, through the choice of one marker per cell, offers total control over the number of SP, with a strong impact on their size and shape if desired.

First, we compute the minima of the gradient g . Each minimum is a connected component, composed of one or more pixels. These minima are truncated along the grid, *i.e.* pixels which fall on the margins between cells are removed.

Second, every cell of the grid serves to define a region of interest in the gradient image. The content of g in this very region is then analyzed to select a unique marker, as explained in the next paragraph.

For each cell, the corresponding marker is chosen among the minima of g which are present in this very cell.

If several minima are present, then the one with the highest surface extinction value [19] is used. We have found surface extinction values to give the best performances compared with volume and dynamic extinction values (data not shown).

It may happen that there is no minimum in a cell. This is an uncommon situation in natural images. In such cases, we must add a marker for the cell which is not a minimum of g , in order to keep regularity. One solution could be to simply choose the center of the cell; however, if this point falls on a local maximum of the gradient g , the resulting SP may coincide with the maximum region and therefore be small in size (leading to a larger variability in size of the SP). We propose instead to take, as marker, the flat zone with minimum value of the gradient inside this very cell.

In both cases (*i.e.* either there exists at least one minimum in the cell or there is not), the selected marker has to be composed of a unique connected component to ensure regularity and connectivity of the resulting superpixel. However, it might not be the case, respectively if more than one minimum

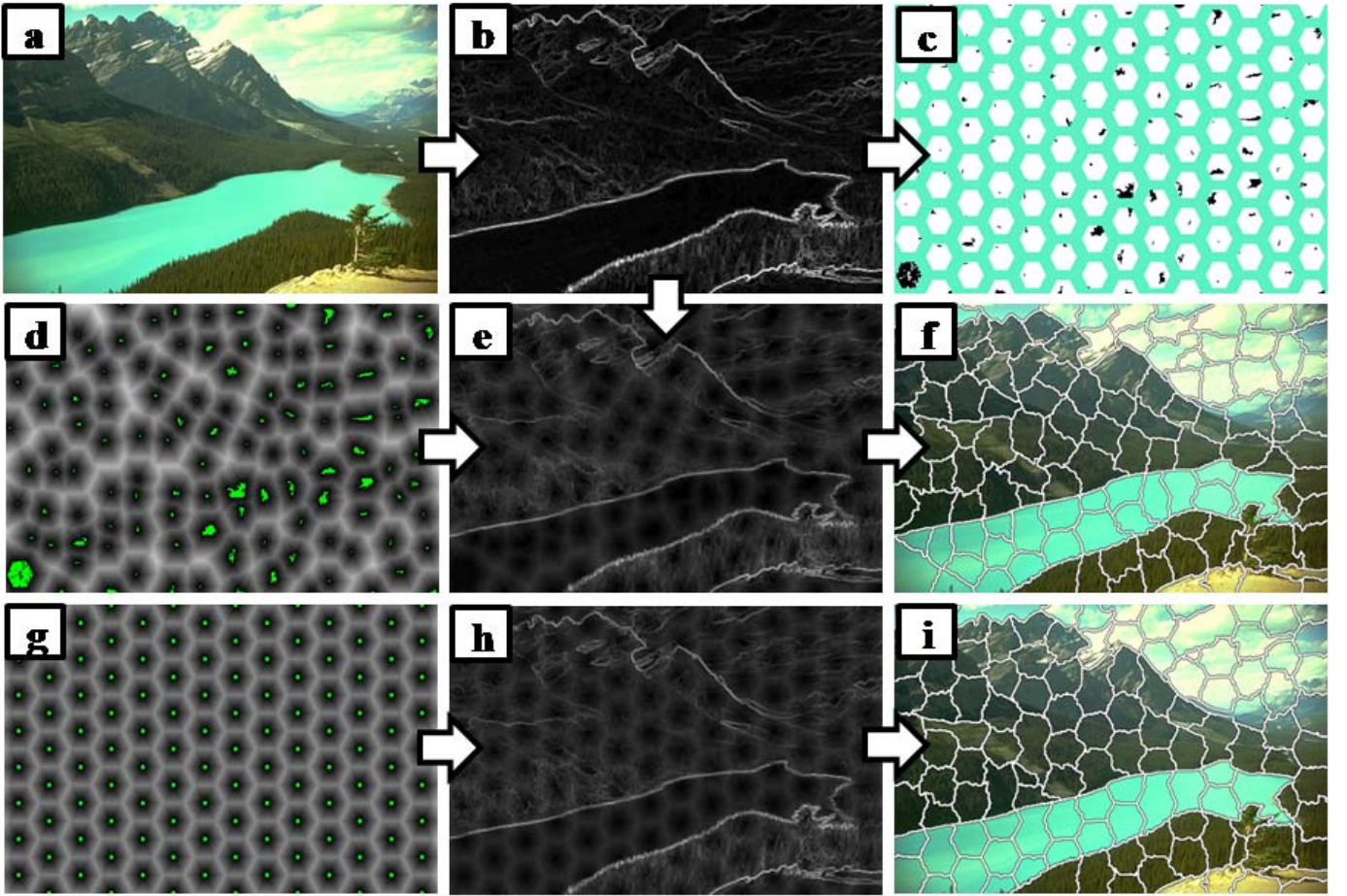


Fig. 2. Illustration of waterpixels generation: (a): original image; (b) corresponding Lab gradient; (c): selected markers within the regular grid of hexagonal cells (step $\sigma = 40$ pixels); (d): distance function to markers; (g): distance function to cell centers; (e) and (h): spatially regularized gradient respectively with distance functions to selected markers (d) and to cell centers (g); (f) and (i): Resulting waterpixels obtained by respectively applying the watershed transformation to (e) and (h), with markers (c).

271 have the same highest extinction value, or if more than one
 272 flat zone present the same lowest gradient value in the cell.
 273 Therefore, an additional step enables to keep only one of
 274 the connected components if there is more than one potential
 275 “best” candidate.

276 The set of resulting markers is denoted $\{M_i\}_{1 \leq i \leq N}$,
 277 $M_i \subset D$. The result of the marker selection procedure is
 278 illustrated in Figure 2.c.

279 C. Spatial Regularization of the Gradient and Watershed

280 The selection of markers has enforced the pertinence of
 281 future superpixel-boundaries but also the regularity of their
 282 pattern (by imposing only one marker per cell). In this
 283 paragraph, we design a spatially regularized gradient in
 284 order to further compromise between boundary adherence and
 285 regularity.

286 Let $Q = \{q_i\}_{1 \leq i \leq N}$ be a set of N connected components
 287 of the image f . For all $p \in D$, we can define a distance
 288 function d_Q with respect to Q as follows:

$$289 \quad \forall p \in D, d_Q(p) = \frac{2}{\sigma} \min_{i \in [1, N]} d(p, q_i) \quad (1)$$

290 where σ is the grid step defined in the previous section. The
 291 normalization by σ is introduced to make the regularization
 292 independent from the chosen SP size.

293 We have studied two possible choices of the q_i . The first one
 294 is to choose them equal to the markers: $q_i = M_i$. Resulting
 295 waterpixels are called m -waterpixels. The second one consists
 296 in setting them at the cell centers: $q_i = o_i$, which leads to
 297 c -waterpixels. We have found that the first gives the best
 298 adherence to object boundaries, while the second produces
 299 more regular superpixels.

300 The spatially regularized gradient g_{reg} is defined as follows:

$$301 \quad g_{reg} = g + kd_Q \quad (2)$$

302 where g is the gradient of the image f , d_Q is the distance
 303 function defined above and k is the spatial regularization
 304 parameter, which takes its values within \mathfrak{R}^+ . The choice of k is
 305 application dependent: when k equals zero, no regularization
 306 of the gradient is applied; when $k \rightarrow \infty$, we approach the
 307 Voronoi tessellation of the set $\{q_i\}_{1 \leq i \leq N}$ in the spatial domain.

308 In the final step, we apply the watershed transformation on
 309 the spatially regularized gradient g_{reg} , starting the flooding
 310 from the markers $\{M_i\}_{1 \leq i \leq N}$, so that an image partition
 311 $\{s_i\}_{1 \leq i \leq N}$ is obtained. The s_i are the resulting waterpixels.

IV. EXPERIMENTS

In order to evaluate waterpixels, the proposed method has been applied on the Berkeley segmentation database [20] and benchmarked against the state-of-the-art. This database is divided into three subsets, “train”, “test” and “val”, containing respectively 200, 200 and 100 images of sizes 321×481 or 481×321 pixels. Approximately 6 human-annotated ground-truth segmentations are given for each image. These ground-truth images correspond to manually drawn contours.

A. Implementation

We have found that it is beneficial to pre-process the images from the database using an area opening followed by an area closing, both of size $\sigma^2/16$ (where σ is the chosen step size of the regular grid). This operation efficiently removes details which are clearly smaller than the expected waterpixel area and which should therefore not give rise to a superpixel contour.

The Lab-gradient is adopted here in order to best reflect our visual perception of color differences and hence the pertinence of detected objects. The margin parameter ρ , described in III-A, is set to $\frac{2}{3}$.

The cell centers correspond to the vertices of a square or an hexagonal grid of step σ . The grid is computed in one pass over the image, by first calculating analytically the coordinates of the set of pixels belonging to each cell and then assigning to them the label of their corresponding cell. We will display the results for the hexagonal grid, as hexagons are more isotropic than squares. Interestingly, they also lead to a better quantitative performance, which was intuitively expected.

The implementation of the waterpixels was done using the Simple Morphological Image Library (SMIL) [21]. SMIL is a Mathematical Morphology library that aims to be fast, lightweight and portable. It brings most classical morphological operators re-designed in order to take advantage of recent computer features (SIMD, parallel processing, ...) to allow handling of very large images and real time processing.

B. Qualitative Analysis

Figure 3 shows various images from the Berkeley segmentation database and their corresponding waterpixels (m -waterpixels and c -waterpixels, hexagonal and square grids, different steps). Figures 3.b and 3.c (zooms of original image presented in 3.a for m -waterpixels and c -waterpixels respectively) show the influence of the regularization parameter k (0, 4, 8, 16) for an homogeneous (blue sky) and a textured (orange rock) regions. As expected, when $k \rightarrow \infty$, m -waterpixels tend towards the Voronoi tessellation of the markers, while c -waterpixels approach the regular grid of hexagonal cells. Both show good adherence to object boundaries, as shown in Figures 3.d, 3.e, 3.f. Of course, enforcing regularity decreases the adherence to object boundaries (see the zoom in Figure 3.f for $k = 16$). One advantage of waterpixels is that the user can choose the shape (and size) of resulting superpixels depending on the application requisites. Figure 3.d, for example, presents waterpixels for hexagonal (second and third columns) and square (fourth column) grids.

As a gradient-based approach, the quality of the watershed is dependant on the borders contrast. If we look at the contours

of objects missed by waterpixels, we see that it is due to the weakness of the gradient, as illustrated in Figure 4.

C. Evaluation Criteria

SP methods produce an image partition $\{s_i\}_{1 \leq i \leq N}$. In order to compute the SP borders, we use a morphological gradient with a 4 neighborhood. Note that the resulting contours are two pixels wide. To this set S_c , we add the one pixel wide image borders S_b . The final set is denoted C . The ground truth image corresponding to the contours of the objects to be segmented, provided in the Berkeley segmentation database, is called GT .

In superpixel generation, we look for an image decomposition into regular regions that adhere well to object boundaries. We propose to use three measures to evaluate this trade-off, namely boundary-recall, contour density and average mismatch factor, as well as computation time.

There are two levels of regularity: (1) the number of pixels required to describe the SP contours, which can be seen as a measure of complexity of individual SP, and (2) the similarity in size and shape between SP.

The first property is evaluated by the Contour Density, which is defined as the number of SP contour pixels divided by the total number of pixels in the image:

$$CD = \frac{\frac{1}{2}|S_c| + |S_b|}{|D|} \quad (3)$$

Note that $|S_c|$ is divided by 2 since contours are two-pixel-wide.

The second property, *i.e.* similarity in size and shape, is evaluated by an adapted version of the mismatch factor [22]. The mismatch factor measures the shape and size dissimilarity between two regions. Given two sets, A and B , the mismatch factor mf between them is defined as:

$$\begin{aligned} mf(A, B) &:= \frac{|A \cup B \setminus A \cap B|}{|A \cup B|} \\ &= 1 - \frac{|A \cap B|}{|A \cup B|} \end{aligned} \quad (4)$$

The mismatch factor and the Jaccard index thus sum to one. Aiming to measure the superpixel regularity, we adapted the mismatch factor to estimate the spread of size and shape distribution. Hence, the average mismatch factor MF is proposed as:

$$MF = \frac{1}{N} \sum_{i=1}^N mf(s_i^*, \hat{s}^*) \quad (5)$$

where s_i^* is the centered version of superpixel s_i , and \hat{s}^* is the average centered shape of all superpixels. The complete definition of the average mismatch factor is given in Appendix.

Note that although compactness is sometimes used in superpixels evaluation (see [23]), it is a poor measurement for region regularity. For example, perfectly-rectangular regions are regular but not compact (because they are different from discs). Waterpixels can in principle tend towards differently shaped superpixels (rectangles, hexagons or other), depending on the grid and the regularization function used. Since the average mismatch factor compares each superpixel against an

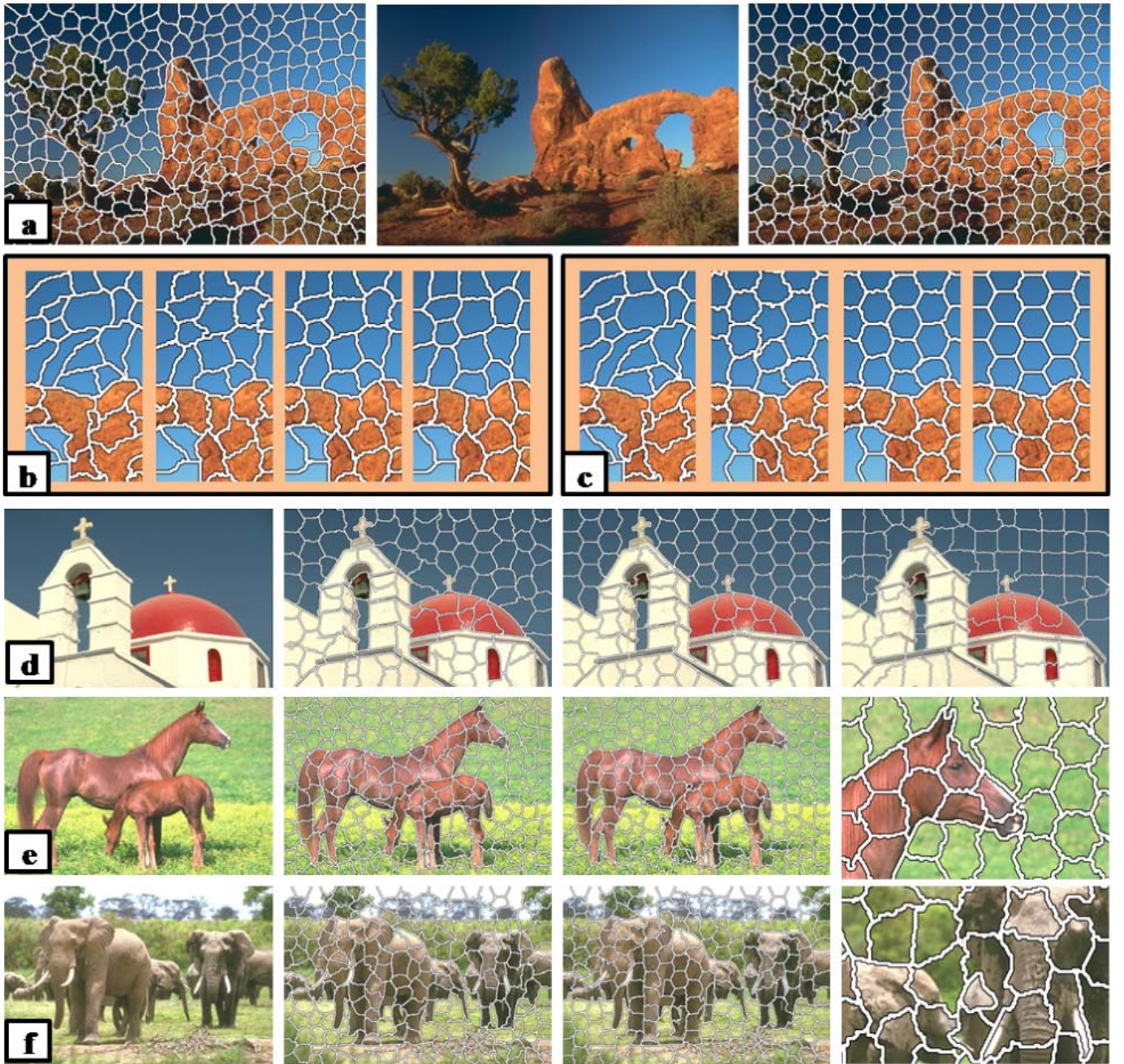


Fig. 3. Illustrations of waterpixels on the Berkeley segmentation database: All waterpixels images are computed with an hexagonal grid with step $\sigma = 30$ pixels and a regularization parameter $k = 8$, unless otherwise specified. (a): original image (middle) with corresponding *m-waterpixels* (left) and *c-waterpixels* (right). $\sigma = 25$ pixels, $k = 16$. (c): zooms of *m-waterpixels* (a) for $k = 0, 4, 8, 16$. (c): zooms of *c-waterpixels* (a) for $k = 0, 4, 8, 16$. (d): original image - *m-wat.* - *c-wat.* - *m-wat.* with square grid and $\sigma = 40$ pixels. (e): original image - *m-wat.* - *c-wat.* - zoom of *c-wat.*. (f): original image - *m-wat.* - *c-wat.* - zoom of *m-wat.* with $k = 16$.

418 image dependent template, this measure is more appropriate
419 to evaluate regularity than compactness.

420 To quantify the adherence to object boundaries, a classical
421 measure used in the literature is the boundary-recall (BR).
422 Boundary-recall is defined as the percentage of ground-truth
423 contour pixels GT which fall within strictly less than 3 pixels
424 from superpixel boundaries C :

$$425 \quad BR = \frac{|\{p \in GT, d(p, C) < 3\}|}{|GT|} \quad (6)$$

426 where d is the L_1 (or Manhattan) distance.

427 While precision cannot be directly used in the context of
428 over-segmentations, boundary-recall has to be, in this partic-
429 ular case of superpixels, interpreted with caution. Indeed, as
430 noted also by Kalinin and Sirota [24], very tortuous contours
431 systematically lead to better performances: because of their
432 higher number, SP contour pixels have a higher chance of
433 matching a true contour, increasing artificially the boundary-
434 recall. Hence, we propose to always consider the trade-off
435 between boundary-recall and contour density to properly
436 evaluate the adherence to object boundaries, penalizing at the
437 same time the cost in pixels to describe SP contours.

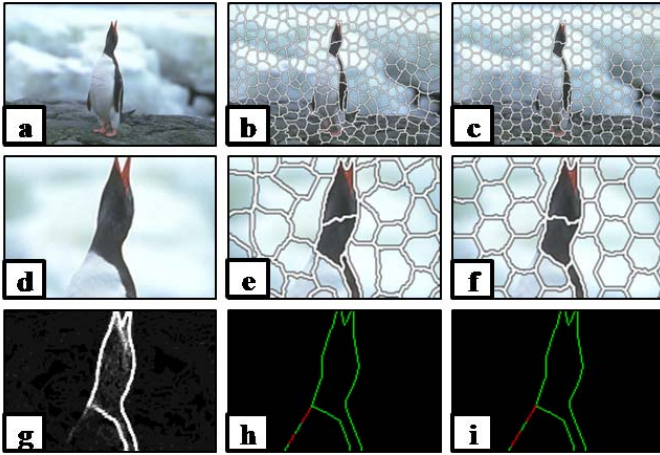


Fig. 4. Contours missed by waterpixels: (a): original image from the Berkeley segmentation database. (b): m -waterpixels with $step = 27$ and $k = 10$. (c): c -waterpixels with $step = 27$ and $k = 10$. (d), (e), (f): zoom of (a), (b), (c) respectively. (g): zoom of the non-regularized gradient image. (h) and (i): reached (green) and missed (red) contours, respectively by m -waterpixels and c -waterpixels.

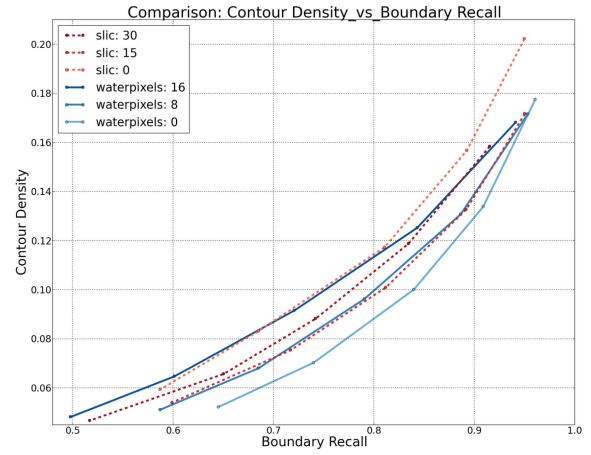
438 *D. Quantitative Analysis and Comparison*
 439 *With State-of-the-Art*

440 In this paragraph, we will use m -waterpixels and denote
 441 them directly as “waterpixels” for the sake of simplicity.

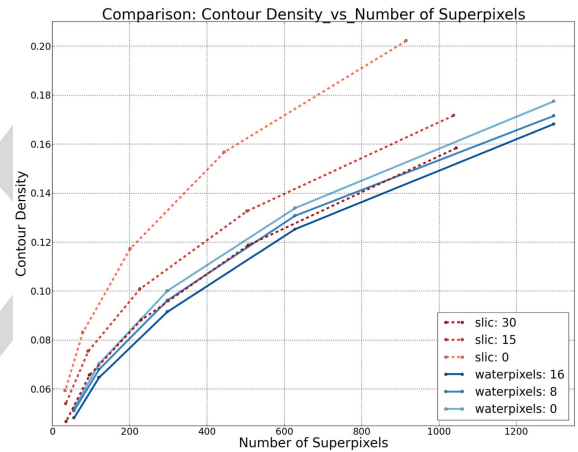
442 During the design of the algorithm, we used intermedi-
 443 ate results from the train and test subsets of the Berkeley
 444 database. Therefore, we report the results obtained for the
 445 validation subset (“val”), which contains 100 images. Results
 446 for boundary-recall, average mismatch factor and contour
 447 density are averaged for this subset and shown in Figure 5.
 448 Blue and red curves correspond to varying regularization
 449 parameters k and k' respectively for waterpixels and SLIC.
 450 The values for k and k' have been chosen such that they
 451 cover a reasonable portion of the regularization space between
 452 no regularization ($k = 0$) and a still acceptable level of
 453 regularization.

454 Figure 5(a) shows contour density against boundary-recall
 455 for waterpixels and SLIC. The ideal case being the lowest con-
 456 tour density for the highest boundary-recall, we can see that
 457 the trade-off between both properties improves for decreasing
 458 regularization, as expected. On the other hand, SLIC shows
 459 another behavior: the trade-off improves, then gets worse
 460 with regularization. At any rate, it is important to note that
 461 waterpixels achieves a better “best” trade-off than SLIC
 462 (see waterpixel $k = 0$ and SLIC $k' = 15$). Besides, this obser-
 463 vation is valid for the whole family of waterpixel-methods as
 464 the zero-value regularization does not take into account d_Q .
 465 In order to do a fair comparison between waterpixels and
 466 SLIC over all criteria, we choose corresponding curves in the
 467 trade-off contour density/boundary-recall, *i.e.* waterpixels with
 468 $k = 8$ and SLIC with $k' = 15$, and compare this couple for
 469 the other criteria.

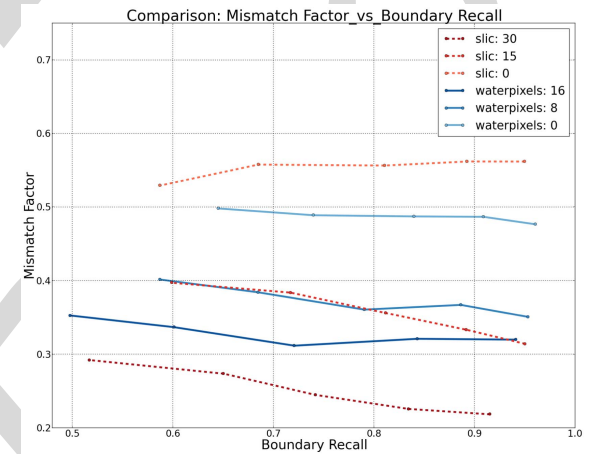
470 Figure 5(b) shows that, for a given number of superpixels,
 471 contour density of waterpixels is more stable and most of
 472 the time lower than SLIC when varying regularization. More
 473 particularly, contour density is lower for waterpixels ($k = 8$)



(a)



(b)



(c)

Fig. 5. Benchmark: performance comparison between waterpixels and SLIC. (a) Contour Density against Boundary-recall. (b) Contour Density against Number of Superpixels. (c) Mismatch factor against Boundary-recall.

474 than for SLIC ($k' = 15$). This means that for the same number
 475 of superpixels, waterpixels contours are shorter than SLIC
 476 contours, which is partly explained by less tortuous contours.

477 Figure 5(c) shows average mismatch factor against
 478 boundary-recall for waterpixels and SLIC. We can see that
 479 the curves for waterpixels with $k = 8$ and SLIC with $k' = 15$
 480 are here again close to each other. 480

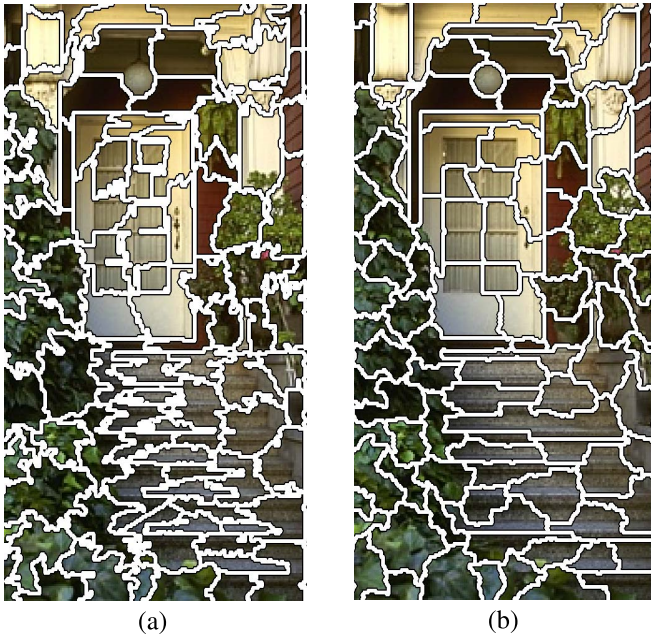


Fig. 6. Comparison between Waterpixels and SLIC superpixels for $\sigma = 25$ pixels on a zoom of an image from the Berkeley segmentation database. (a) SLIC $k' = 15$. (b) Waterpixels $k = 8$.

481 These properties are illustrated in Figure 6, where we can
 482 see examples of reached and missed contours by both methods,
 483 as well as their different behaviours in terms of regularity
 484 (shape, size, tortuosity).

485 E. Computation Time

486 Computing time was measured on a personal computer
 487 based on Intel(R) Core(TM) i7 central processing units
 488 (4 physical cores, 4 virtual ones), operating at 2.93GHz. Both
 489 methods have linear complexity with the number of pixels in
 490 the image. For an image of size 481×321 , average computing
 491 time for SLIC was 149 ms, and 132 ms for waterpixels
 492 (82 ms without pre-filtering). A more detailed comparison of
 493 computation times is presented in Figure 7 (showing average
 494 and standard deviation for different numbers of superpixels).
 495 We can see that waterpixels are generally faster to compute
 496 than SLIC superpixels. Contrary to the latter's, their compu-
 497 tation time decreases slightly with the number of superpixels.
 498 An analysis of computation times for the different steps of
 499 waterpixels reveals that this variability is only introduced by
 500 the grid computation and the minima selection procedure.
 501 Concerning grid computation time, it rises from 2 ms for
 502 small numbers of waterpixels to 27 ms for large numbers of
 503 waterpixels. This simply means that we still have to optimize
 504 this step. Concerning the computation time of the minima
 505 selection procedure, it decreases as waterpixels become larger
 506 because of pre-filtering step. Indeed, the size of this filtering
 507 is directly proportional to the cell size. As such, resulting
 508 images contain less minima, which simplifies the selection
 509 procedure. Besides, the variance observed when we change
 510 images is explained by the fact that the difficulty of minima
 511 evaluation/computation depends on the content of each image.

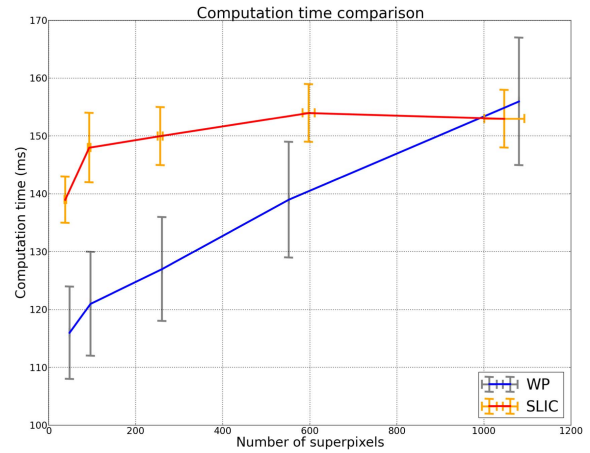


Fig. 7. Computation time comparison with images of the Berkeley database.

We are currently working on a new implementation of minima
 computation/evaluation which would be less dependent on the
 number of superpixels.

To conclude this section, waterpixels are generally faster
 to compute than SLIC superpixels, and they are at least
 as performant in the trade-off between adherence to object
 boundaries and regularity in shape and size, while using much
 less pixels to describe their contours.

V. DISCUSSION AND PERSPECTIVES

We have shown that waterpixels produce competitive results
 with respect to the state-of-the-art. These advantages are
 valuable in the classification/detection/segmentation pipeline,
 where superpixels play the part of primitives. Moreover, there
 is one major difference in the construction of the algorithm:
 the SLIC approach does not impose any connectivity con-
 straint. The resulting superpixels are therefore not necessarily
 connected, which requires some *ad hoc* postprocessing step.
 In contrast, waterpixels are connected by definition, and the
 connectivity constraint is actually implemented in the distance
 used.

The proposed approach is gradient-based. Standard methods
 can be used to compute this gradient, or a specific gradient
 computation method can be designed for a given application.
 In any case, this offers flexibility to waterpixels. One limitation
 though is the quality of the signal in such a gradient image.
 As seen in 4, alteration by noise or insufficiently contrasted
 contours may lead to the prevalence of regularity over adher-
 ence to object boundaries. If filtering steps are usually enough
 to deal with noise and remove non pertinent small details,
 parameter values have to be optimized for each database.
 Future work will aim at overcoming this limitation by adding a
 learning step of optimal filtering values for specific databases.

The general design of waterpixels offers many prospects.
 Among them, one promising field of improvement resides
 in the placement of markers, as they constitute the main
 degree of freedom of the method. We are currently investi-
 gating the possibility to select the markers in an optimal
 manner, for example by formulating the marker placement as a
 p -dispersion problem (see [25]) in an augmented space.

551 The speed of waterpixels contributes to expanding their
 552 possible applications. For example, it could be interest-
 553 ing to compute different sets of waterpixels, by changing
 554 design options (different cells, gradients, grid steps, etc.),
 555 and then use ensemble clustering methods to obtain a final
 556 segmentation [26], [27].

557 Last but not least, waterpixels lead to the efficient construc-
 558 tion of hierarchical partitions based on superpixels. Indeed,
 559 the computation of the watershed can produce at the same
 560 time a segmentation and a hierarchy of partitions based on
 561 that segmentation, with only minor overhead computation
 562 times [28]–[30].

563 VI. CONCLUSION

564 This paper introduces waterpixels, a family of methods
 565 for computing regular superpixels based on the watershed
 566 transformation. Both adherence to object boundaries and regu-
 567 larity of resulting regions are encouraged thanks to the choice
 568 of the markers and the gradient to be flooded. Different
 569 design options, such as the distance function used to spatially
 570 regularized the gradient, lead to different trade-offs between
 571 both properties. The computational complexity of waterpixels
 572 is linear. Our current implementation makes it one of the
 573 fastest superpixel methods. Experimental results show that
 574 waterpixels are competitive with respect to the state-of-the-art.
 575 They outperform SLIC superpixels, both in terms of quality
 576 and speed. The trade-off between speed and segmentation
 577 quality achieved by waterpixels, as well as their ability to
 578 generate hierarchical segmentations at negligible extra cost,
 579 offer interesting perspectives for this superpixels generation
 580 method.

581 An implementation of waterpixels is available from
 582 <http://cmm.ensmp.fr/~machairas/waterpixels>.

583 APPENDIX

584 MEAN MISMATCH FACTOR DEFINITION

585 Let $\{s_i\}_{1 \leq i \leq N}$ be a set of superpixels. The centered version
 586 s_i^* of s_i is obtained by translating s_i so that its barycenter is
 587 the origin of the coordinates system.

588 The average shape \widehat{s}^* of the $\{s_i\}$ is computed as follows.
 589 Let first define function S :

$$590 \quad S : \begin{cases} D & \longrightarrow \mathbb{N} \\ x_p & \longmapsto \sum_{i=1}^N 1_i(x_p) \end{cases} \quad (7)$$

591 where 1_i is the indicator function of s_i^* . Thus, image S cor-
 592 responds to the summation image of all centered superpixels.
 593 Let furthermore $\mu_A = 1/n \sum_{i=1}^N |s_i|$ be the average area of
 594 the considered superpixels, and let S_t be the threshold of S at
 595 level t : $S_t(x) = \{x_p \in D \mid |S(x_p)| \geq t\}$.

596 The average centered shape \widehat{s}^* is then the set S_{t_0} , where t_0
 597 is the maximal threshold value which enables \widehat{s}^* to have an
 598 area greater than or equal to μ_A :

$$599 \quad t_0 = \max\{t \mid |S_t| \geq \mu_A\} \quad (8)$$

$$600 \quad \widehat{s}^* = S_{t_0} \quad (9)$$

601 Finally, the mean mismatch factor of superpixels
 602 $\{s_i\}_{1 \leq i \leq N}$ is:

$$603 \quad MF = \frac{1}{N} \sum_{i=1}^N mf(s_i^*, \widehat{s}^*). \quad (10)$$

604 REFERENCES

- 605 [1] S. Beucher and C. Lantuéjoul, "Use of watersheds in contour detec-
 606 tion," in *Proc. Int. Workshop Image Process., Real-Time Edge Motion*
 607 *Detection/Estimation*, 1979. AQ:5
- 608 [2] S. Beucher and F. Meyer, "The morphological approach to segmentation:
 609 The watershed transformation," in *Mathematical Morphology in Image*
 610 *Processing*, E. Dougherty, Ed. 1993, pp. 433–481. AQ:6
- 611 [3] F. Meyer, "Un algorithme optimal pour la ligne de partage des
 612 eaux," *Dans 8^e Congrès Reconnaissance Formes Intell. Artif.*, vol. 2,
 613 pp. 847–857, Nov. 1991.
- 614 [4] L. Vincent and P. Soille, "Watersheds in digital spaces: An efficient
 615 algorithm based on immersion simulations," *IEEE Trans. Pattern Anal.*
 616 *Mach. Intell.*, vol. 13, no. 6, pp. 583–598, Jun. 1991.
- 617 [5] R. Achanta, A. Shaji, K. Smith, A. Lucchi, P. Fua, and S. Süsstrunk,
 618 "SLIC superpixels compared to state-of-the-art superpixel methods,"
 619 *IEEE Trans. Pattern Anal. Mach. Intell.*, vol. 34, no. 11, pp. 2274–2282,
 620 Nov. 2012.
- 621 [6] V. Machairas, E. Decencière, and T. Walter, "Waterpixels: Superpixels
 622 based on the watershed transformation," in *Proc. IEEE Int. Conf. Image*
 623 *Process. (ICIP)*, Oct. 2014, pp. 4343–4347.
- 624 [7] X. Ren and J. Malik, "An optimal region growing algorithm for image seg-
 625 mentation," *Int. J. Pattern Recognit. Artif. Intell.*, vol. 1, nos. 3–4,
 626 pp. 351–375, 1987. [Online]. Available: <http://www.worldscientific.com/doi/abs/10.1142/S0218001487000242>
- 627 [8] B. Marcotegui and F. Meyer, "Bottom-up segmentation of image
 628 sequences for coding," *Ann. Télécommun.*, vol. 52, nos. 7–8,
 629 pp. 397–407, 1997. [Online]. Available: <http://link.springer.com/article/10.1007/BF02998459>
- 630 [9] X. Ren and J. Malik, "Learning a classification model for segmentation,"
 631 in *Proc. 9th IEEE Int. Conf. Comput. Vis.*, vol. 1, Oct. 2003, pp. 10–17.
- 632 [10] P. F. Felzenszwalb and D. P. Huttenlocher, "Efficient graph-based
 633 image segmentation," *Int. J. Comput. Vis.*, vol. 59, no. 2, pp. 167–181,
 634 Sep. 2004.
- 635 [11] A. Levinstein, A. Stere, K. N. Kutulakos, D. J. Fleet, S. J. Dickinson,
 636 and K. Siddiqi, "TurboPixels: Fast superpixels using geometric flows,"
 637 *IEEE Trans. Pattern Anal. Mach. Intell.*, vol. 31, no. 12, pp. 2290–2297,
 638 Dec. 2009.
- 639 [12] J. Wang and X. Wang, "VCells: Simple and efficient superpixels using
 640 edge-weighted centroidal Voronoi tessellations," *IEEE Trans. Pattern*
 641 *Anal. Mach. Intell.*, vol. 34, no. 6, pp. 1241–1247, Jun. 2012.
- 642 [13] G. Zeng, P. Wang, J. Wang, R. Gan, and H. Zha, "Structure-sensitive
 643 superpixels via geodesic distance," *Int. Conf. Comput. Vis.*, vol. 1, no. 1,
 644 pp. 1–27, 2011.
- 645 [14] O. Veksler, Y. Boykov, and P. Mehrani, "Superpixels and supervoxels in
 646 an energy optimization framework," in *Proc. 11th Eur. Conf. Comput.*
 647 *Vis.*, 2010, pp. 211–224.
- 648 [15] P. Soille, *Morphological Image Analysis: Principles and Applications*.
 649 New York, NY, USA: Springer-Verlag, 2003.
- 650 [16] B. Andres, U. Köthe, M. Helmstaedter, W. Denk, and F. A. Hamprecht,
 651 "Segmentation of SBFSEM volume data of neural tissue by hier-
 652 archical classification," in *Pattern Recognition*, Berlin, Germany:
 653 Springer-Verlag, 2008, pp. 142–152.
- 654 [17] J. Stawiński, E. Decencière, and F. Bidault, "Interactive liver tumor
 655 segmentation using graph cuts and watershed," in *Proc. MICCAI*,
 656 New York, NY, USA, 2008.
- 657 [18] P. Neubert and P. Protzel, "Compact watershed and preemptive SLIC:
 658 On improving trade-offs of superpixel segmentation algorithms," in
 659 *Proc. IEEE 22nd Int. Conf. Pattern Recognit. (ICPR)*, Aug. 2014,
 660 pp. 996–1001.
- 661 [19] C. Vachier and F. Meyer, "Extinction values: A new measurement
 662 of persistence," in *Proc. IEEE Workshop Non Linear Signal/Image*
 663 *Process.*, 1995, pp. 254–257.
- 664 [20] D. Martin, C. Fowlkes, D. Tal, and J. Malik, "A database of human
 665 segmented natural images and its application to evaluating segmentation
 666 algorithms and measuring ecological statistics," in *Proc. 8th IEEE Int.*
 667 *Conf. Comput. Vis.*, vol. 2, Jul. 2001, pp. 416–423.
- 668 [21] M. Faessel and M. Bilodeau, "SMIL: Simple morphological image
 669 library," LRDE, Tech. Rep., 2013.
- 670 AQ:8

- 672 [22] N. J. C. Strachan, P. Nesvadba, and A. R. Allen, "Fish
673 species recognition by shape analysis of images," *Pattern*
674 *Recognit.*, vol. 23, no. 5, pp. 539–544, 1990. [Online]. Available:
675 <http://www.sciencedirect.com/science/article/pii/003132039090074U>
- 676 [23] A. Schick, M. Fischer, and R. Stiefelhagen, "An evaluation of the
677 compactness of superpixels," *Pattern Recognit. Lett.*, vol. 43, pp. 71–80,
678 Jul. 2014.
- 679 [24] P. Kalinin and A. Sirota, "A graph based approach to hierar-
680 chical image over-segmentation," *Comput. Vis. Image Understand.*,
681 vol. 130, pp. 80–86, Jan. 2015. [Online]. Available: <http://www.sciencedirect.com/science/article/pii/S1077314297905464>
- 682 [25] E. Erkut, "The discrete p -dispersion problem," *Eur. J. Oper. Res.*,
683 vol. 46, no. 1, pp. 48–60, May 1990.
- 684 [26] K. Cho and P. Meer, "Image segmentation from consensus informa-
685 tion," *Comput. Vis. Image Understand.*, vol. 68, no. 1, pp. 72–89,
686 Oct. 1997. [Online]. Available: <http://www.sciencedirect.com/science/article/pii/S1077314297905464>
- 687 [27] A. Strehl and J. Ghosh, "Cluster ensembles—A knowledge
688 reuse framework for combining multiple partitions," *J. Mach.*
689 *Learn. Res.*, vol. 3, pp. 583–617, Mar. 2003. [Online]. Available:
690 <http://dx.doi.org/10.1162/153244303321897735>
- 691 [28] F. Meyer, "Minimum spanning forests for morphological segmentation,"
692 in *Mathematical Morphology and Its Applications to Image Processing*.
693 Boston, MA, USA: Kluwer, Sep. 1994, pp. 77–84.
- 694 [29] S. Beucher, "Watershed, hierarchical segmentation and waterfall algo-
695 rithm," in *Mathematical Morphology and Its Applications to Image*
696 *Processing*, J. Serra and P. Soille, Eds. Fontainebleau, France: Kluwer,
697 Sep. 1994, pp. 69–76.
- 698 [30] F. Meyer, "An overview of morphological segmentation," *Int. J. Pattern*
699 *Recognit. Artif. Intell.*, vol. 15, no. 7, pp. 1089–1118, 2001.

702
703
704
705
706
707
708
709
710
711



Vaia Machairas received the Engineering degree in optics from the Institut d'Optique Graduate School (Supoptique), Palaiseau, France, and the master's degree in optics, image, vision from Jean Monnet University, Saint Etienne, France, both in 2013. She is currently pursuing the Ph.D. degree with the Centre for Mathematical Morphology, MINES ParisTech. Her research interests include mathematical morphology, image segmentation, machine learning, and colorimetry.

712
713
714
715
716
717
718



Matthieu Faessel received the Ph.D. degree in engineer sciences from the University of Bordeaux, France, in 2003. He is currently a Research Engineer with the Centre of Mathematical Morphology, School of Mines, Paris, France. His research interests include image segmentation, computer vision, and materials.



David Cárdenas-Peña received the bachelor's degree in electronic engineering and the M.Eng. degree in industrial automation from the Universidad Nacional de Colombia, Manizales-Colombia, in 2008 and 2011, respectively. He is currently pursuing the Ph.D. degree in automatics with the Universidad Nacional de Colombia. He has been a Research Assistant with the Signal Processing and Recognition Group since 2008. His current research interests include machine learning and signal and image processing.

719
720
721
722
723
724
725
726
727
728
729



Théodore Chabardes received the degree from the Engineering School, ESIEE Paris, France, in 2014, as an Engineer specialized in computer science. He is currently pursuing the Ph.D. degree with the Centre of Mathematical Morphology, School of Mines, Paris, France. His research interests include mathematical morphology, image segmentation, and software optimization.

730
731
732
733
734
735
736
737



Thomas Walter received the Diploma degree in electrical engineering from Saarland University, Germany, and the Ph.D. degree in mathematical morphology from Mines ParisTech, France. He held a post-doctoral position with the European Molecular Biology Laboratory, Heidelberg, Germany. He is currently a Team Leader in bioimage informatics with the Centre for Computational Biology, Mines ParisTech, and a member of the Bioinformatics Unit with the Curie Institute, Paris. His most visible scientific contributions have been in the field of bioimage informatics, and in particular, in high content screening. He has pioneered methods in the field of cellular phenotyping and phenotypic clustering from live cell-imaging data. He was involved in the first genome-wide screen by live cell imaging in a human cell line, and co-develops the open-source software cellcognition.

738
739
740
741
742
743
744
745
746
747
748
749
750
751
752
753



Etienne Decencière received the Engineering degree and the Ph.D. degree in mathematical morphology from MINES ParisTech, France, in 1994 and 1997, respectively, and the Habilitation à Diriger des Recherches from Jean Monnet University, in 2008. He holds a research fellow position with the Centre for Mathematical Morphology, MINES ParisTech, where he leads several academic and industrial research projects. His main research interests are in mathematical morphology, image segmentation, and biomedical applications.

754
755
756
757
758
759
760
761
762
763
764

AUTHOR QUERIES

AQ:1 = Please check whether the edits made in the financial section are OK.

AQ:2 = Please confirm the current affiliation of all authors.

AQ:3 = Please confirm the postal code for “MINES ParisTech, PSL Research University, Center for Mathematical Morphology, Universidad Nacional de Colombia, Centre for Computational Biology, Institut Curie, and Inserm.”

AQ:4 = Table I is not cited in body text. Please indicate where it should be cited.

AQ:5 = Please provide the page range for ref. [1].

AQ:6 = Please provide the publisher name and location for ref. [2].

AQ:7 = Please provide the page range and also confirm the conference title for ref. [17].

AQ:8 = Please provide the organization, location, and report no. for ref. [21].

IEEE
Proof

Waterpixels

Vaia Machairas, Matthieu Faessel, David Cárdenas-Peña, Théodore Chabardes,
Thomas Walter, and Etienne Decencière

1 **Abstract**—Many approaches for image segmentation rely on a
2 first low-level segmentation step, where an image is partitioned
3 into homogeneous regions with enforced regularity and adherence
4 to object boundaries. Methods to generate these superpixels have
5 gained substantial interest in the last few years, but only a few
6 have made it into applications in practice, in particular because
7 the requirements on the processing time are essential but are not
8 met by most of them. Here, we propose waterpixels as a general
9 strategy for generating superpixels which relies on the marker
10 controlled watershed transformation. We introduce a spatially
11 regularized gradient to achieve a tunable tradeoff between the
12 superpixel regularity and the adherence to object boundaries.
13 The complexity of the resulting methods is linear with respect
14 to the number of image pixels. We quantitatively evaluate our
15 approach on the Berkeley segmentation database and compare
16 it against the state-of-the-art.

17 **Index Terms**—Superpixels, watershed, segmentation.

I. INTRODUCTION

18
19 **SUPERPIXELS** (SP) are regions resulting from
20 a low-level segmentation of an image and are typically
21 used as primitives for further analysis such as detection,
22 segmentation, and classification of objects (see Figure 1
23 for an illustration). The underlying idea is that this first
24 low-level partition alleviates the computational complexity of
25 the following processing steps and improves their robustness,
26 as not single pixel values but pixel set features can be used.

27 Superpixels should have the following properties:

28 1) **homogeneity**: pixels of a given SP should present
29 similar colors or gray levels;

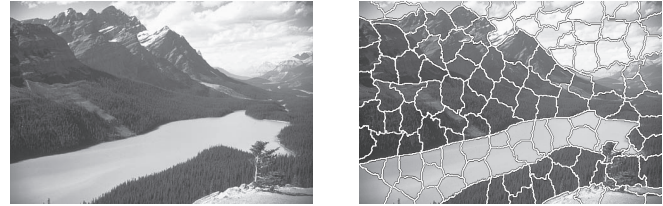


Fig. 1. Superpixels illustration. The original image comes from the Berkeley segmentation database. (a) Original image. (b) Waterpixels.

- 30 2) **connected partition**: each SP is made of a single
31 connected component and the SPs constitute a partition
32 of the image;
- 33 3) **adherence to object boundaries**: object boundaries
34 should be included in SP boundaries;
- 35 4) **regularity**: SPs should form a regular pattern on the
36 image. This property is often desirable as it makes the
37 SP more convenient to use for subsequent analysis steps.

38 The requirements on regularity and boundary adherence
39 are to a certain extent oppositional, and a good solution
40 typically aims at finding a compromise between these two
41 requirements.

42 In addition to these requirements on superpixel quality,
43 computational efficiency is an absolutely essential aspect, as
44 the partition into superpixels is typically only the first step of
45 an often complex and potentially time consuming workflow.
46 Methods of linear complexity are consequently of particular
47 interest.

48 We therefore hypothesized that the Watershed transforma-
49 tion [1], [2] should be an interesting candidate for superpixel
50 generation, as it has been shown to achieve state-of-the-art
51 performance in many segmentation problems, it is
52 non-parametric, and there exist linear-complexity algorithms
53 to compute it, as well as efficient implementations [3], [4].
54 The only often cited drawback, oversegmentation, does not
55 seem to be problematic for superpixel generation, as long as
56 we can control the degree of oversegmentation (number of
57 superpixels), and the regularity of the resulting partition.

58 Given these considerations, we propose a strategy for
59 applying the watershed transform to superpixel generation,
60 where we use a spatially regularized gradient to achieve a
61 tunable trade-off between superpixel regularity and adherence
62 to object boundaries. We quantitatively evaluate our method
63 on the Berkeley segmentation database and show that we
64 outperform the best linear-time state-of-the-art method: Simple
65 Linear Iterative Clustering (SLIC) [5]. We call the resulting
66 superpixels “waterpixels.”

AQ:1 Manuscript received December 18, 2014; revised April 17, 2015; accepted
June 15, 2015. The work of T. Walter was supported by the European
Community through the Seventh Framework Programme (FP7/2007-2013)
within the Systems Microscopy under Grant 258068. The associate editor
coordinating the review of this manuscript and approving it for publication
was Dr. Yonggang Shi.

AQ:2 V. Machairas, M. Faessel, T. Chabardes, and E. Decencière are with
AQ:3 MINES ParisTech, Paris 75006, France, also with PSL Research University,
Paris 75005, France, and also with the Center for Mathematical Morphology,
Fontainebleau 77305, France (e-mail: vaia.machairas@mines-paristech.fr;
matthieu.faessel@mines-paristech.fr; theodore.chabardes@mines-paristech.fr;
etienne.decenciere@mines-paristech.fr).

D. Cárdenas-Peña is with the Signal Processing and Recognition Group,
Universidad Nacional de Colombia, Manizales 170001-17, Colombia (e-mail:
dcardenas@unal.edu.co).

T. Walter is with MINES ParisTech, Paris 75006, France, also with PSL
Research University, Paris 75005, France, also with the Centre for Compu-
tational Biology, Fontainebleau 77305, France, also with the Institut Curie,
Paris 75248, France, and also with Inserm, Paris 75248, France (e-mail:
thomas.walter@mines-paristech.fr).

Color versions of one or more of the figures in this paper are available
online at <http://ieeexplore.ieee.org>.

Digital Object Identifier 10.1109/TIP.2015.2451011

TABLE I
 RECAP CHART OF EXISTING METHODS TO COMPUTE REGULAR
 SUPERPIXELS (n IS THE NUMBER OF PIXELS IN THE IMAGE; i IS
 THE NUMBER OF ITERATIONS REQUIRED; N THE NUMBER
 OF SUPERPIXELS). “WP” CORRESPONDS TO OUR
 METHOD, CALLED “WATERPIXELS”

Method	[11]	[12]	[13]	[5]	WP
Generation type (see section II-B)	1	2	1 (iterated)	2	1
Seed type (see section II-A)	A	C	C	C	B
Control on number of SPs	yes	yes	yes	no	yes
Control on regularity	no	yes	no	yes	yes
Post-processing free	no	no	no	no	yes
Complexity	$O(n)$	$O(in\sqrt{N})$	$O(in)$	$O(n)$	$O(n)$

This paper is an extended version of [6]. It proposes a more general approach (elaborating a whole family of waterpixels generation methods), with a more thorough validation and improved results with regard to the trade-off between boundary adherence and regularity, as well as computation time. Moreover, we have developed and made available a fast implementation of waterpixels.

II. RELATED WORK

Low-level segmentations have been used for a long time as first step towards segmentation [7], [8]. The term superpixel was coined much later [9], albeit in a more constrained framework. This approach has raised increasing interest since then. Various methods exist to compute SPs, most of them based on graphs [10], geometrical flows [11] or k-means [5]. We will focus on linear complexity methods generating regular SPs.

Methods for SP generation are all based on two steps: an initialization step where either seeds or a starting partition are defined and a (potentially iterative) assignment step, where each pixel is assigned to one superpixel, starting from the initialization. In the next section, we are going to review previously published approaches for SP generation with respect to these aspects and compare them regarding various performance criteria. We limit the presentation of existing methods to those with linear complexity.

A. Choosing the Seeds

In the first step, a set of seeds is chosen, which are typically spaced regularly over the image plane and which can be either regions or single pixels:

- Type A seeds are independent of the image content. These are typically the cells or the centers of a regular grid.
- Type B seeds depend on the content of the image (compromise between a regular cover of the image plane and an adaption to the contour).
- Type C seeds are initially image independent, then they are iteratively refined to take into account the image contents.

If the seed does not depend on the image, an iterative refinement is usually preferable, and therefore more time

is spent on the computation of the SP. Type B methods may spend more time on finding appropriate seeds, but can therefore afford not to iterate the SP generation.

B. Building Superpixels From Seeds

In the second step, the partition into superpixels is built from the seeds. Among the methods with linear complexity, there are two main strategies for this:

Shortest Path Methods (Type 1) [11], [13]: these methods are based on region growing: they start from a set of seeds (points or regions) and successively extend them by incorporating pixels in their neighborhood according to a usually image dependent cost function until every pixel of the image plane has been assigned to exactly one superpixel. This process may or may not be iterated.

Shortest Distance Methods (Type 2) [5], [12]: these are iterative procedures inspired by the field of unsupervised learning, where at each iteration step, seeds (such as centroids) are calculated from the previous partition and pixels are then re-assigned to the closest seed (like for example the k -means approach).

Even though methods inspired by general clustering methods (type 2) seem appealing at first sight, in particular when they globally optimize a cost function, this class of methods does not guarantee connectivity of the superpixels for arbitrary choices of the pixel-seed distance (see [5], [12]). For instance, the distance metric proposed in [5] (a combination of Euclidean and grey level distance), leads to non-connected superpixels, which is undesirable. To solve this issue, a post-processing step is necessary, consisting either in relabeling the image so that every connected component has its own label (see [12]), leading to a more irregular distribution of SP sizes and shapes, or in reassigning isolated regions to the closest and large enough Superpixel, as in [5], leading to non-optimality of the solution and an unpredictable number of superpixels. In addition, such postprocessing increases the computational cost and can turn out to be the most time-consuming step when the image contains numerous small objects/details compared to the size of the Superpixel.

On the contrary, methods based on region growing (type 1) inherently implement a “path-type” distance, where the distance between two pixels does not only depend on value and position of the pixels themselves, but on values and positions along the path connecting them. Type 1 methods imply connected superpixel regions, for which the number of superpixels is exactly the number of seeds.

C. Other Properties

It is generally accepted that a good superpixel-generation method should provide to the user total control over the number of resulting Superpixels. While this property is achieved by [11]–[14], some only reach approximatively this number because of post-processing (either by splitting too big superpixels, or removing small isolated superpixels as in [5]). Another parameter is the control on superpixels regularity in the trade-off between regularity and adherence to contours. Only [5] and [12] enable the user to weight the importance

of regularity compared to boundary adherence, so it can be adapted to the application.

As far as performance is concerned, one of the main criteria is undoubtedly the complexity that the method requires. Indeed, for Superpixels to be used as primitives for further analysis such as classification, their computation should neither take too long nor too much memory. This is the reason why we focus on linear complexity methods. Among them, SLIC appears to offer the best performance with regards to the trade-off between adherence to boundaries and regularity [5]. Moreover, since its recent inception, this method has become very popular in the computer vision community. We will therefore use it as reference for the quantitative evaluation of our method.

D. Superpixels and Watershed

In principle, the watershed transformation (see [15] for a review) is well suited for SP generation:

- 1) It gives a good adherence to object boundaries when computed on the image gradient.
- 2) It allows to control the number and spatial arrangement of the resulting regions through the choice of markers.
- 3) The connectivity of resulting regions is guaranteed and no postprocessing is required.
- 4) It offers linear complexity with the number of pixels in the image.

Indeed, it has been used to produce low-level segmentations in several applications, including computation intensive 3D applications [16], [17], in particular when shape regularity of the elementary regions was not required.

Previous publications claimed that the watershed transformation does not allow for the generation of spatially regular SP [5], [11]. Recently, we and others [6], [18] have shown that in principle the watershed transformation can be applied to SP generation.

Here, we introduce waterpixels, a family of methods based on the watershed transformation to compute superpixels.

III. WATERPIXELS

As most watershed-based segmentation methods, waterpixels are based on two steps: the definition of markers, from which the flooding starts, and the definition of a gradient (the image to be flooded). We propose to design these steps in such a way that regularity is encouraged.

A waterpixel-generation method is characterized by the following steps:

- 1) Computation of the gradient of the image;
- 2) Definition of regular cells on the image, centered on the vertices of a regular grid;
- 3) Selection of one marker per cell;
- 4) Spatial regularization of the gradient with the help of a distance function;
- 5) Application of the watershed transformation on the regularized gradient defined in step 4 from the markers defined in step 2.

These steps are illustrated in figure 2 and developed in the next paragraphs.

A. Gradient and Cells Definition

Let $f : D \rightarrow V$ be an image, where D is a rectangular subset of Z^2 , and V a set of values, typically $\{0, \dots, 255\}$ when f is a grey level image, or $\{0, \dots, 255\}^3$ for color images.

The first step consists in computing the gradient image g of the image f . The choice of the gradient operator depends on the image type, *e.g.* for grey level images we might choose a morphological gradient. This gradient will be used to choose the seeds (section III-B) and to build the regularised gradient (III-C).

For the definition of cells, we first choose a set of N points $\{o_i\}_{1 \leq i \leq N}$ in D , called *cell centers*, so that they are placed on the vertices of a regular grid (a square or hexagonal one for example). Given a distance d on D , we denote by σ the grid step, *i.e.* the distance between closest grid points.

A Voronoi tessellation allows to associate to each o_i a Voronoi cell. For each such cell, a homothety centered on o_i with factor ρ ($0 < \rho \leq 1$) leads to the computation of the final cell C_i . This last step allows for the creation of a margin between neighbouring cells, in order to avoid the selection of markers too close from each other.

B. Selection of the Markers

As each cell is meant to correspond to the generation of a unique waterpixel, our method, through the choice of one marker per cell, offers total control over the number of SP, with a strong impact on their size and shape if desired.

First, we compute the minima of the gradient g . Each minimum is a connected component, composed of one or more pixels. These minima are truncated along the grid, *i.e.* pixels which fall on the margins between cells are removed.

Second, every cell of the grid serves to define a region of interest in the gradient image. The content of g in this very region is then analyzed to select a unique marker, as explained in the next paragraph.

For each cell, the corresponding marker is chosen among the minima of g which are present in this very cell.

If several minima are present, then the one with the highest surface extinction value [19] is used. We have found surface extinction values to give the best performances compared with volume and dynamic extinction values (data not shown).

It may happen that there is no minimum in a cell. This is an uncommon situation in natural images. In such cases, we must add a marker for the cell which is not a minimum of g , in order to keep regularity. One solution could be to simply choose the center of the cell; however, if this point falls on a local maximum of the gradient g , the resulting SP may coincide with the maximum region and therefore be small in size (leading to a larger variability in size of the SP). We propose instead to take, as marker, the flat zone with minimum value of the gradient inside this very cell.

In both cases (*i.e.* either there exists at least one minimum in the cell or there is not), the selected marker has to be composed of a unique connected component to ensure regularity and connectivity of the resulting superpixel. However, it might not be the case, respectively if more than one minimum

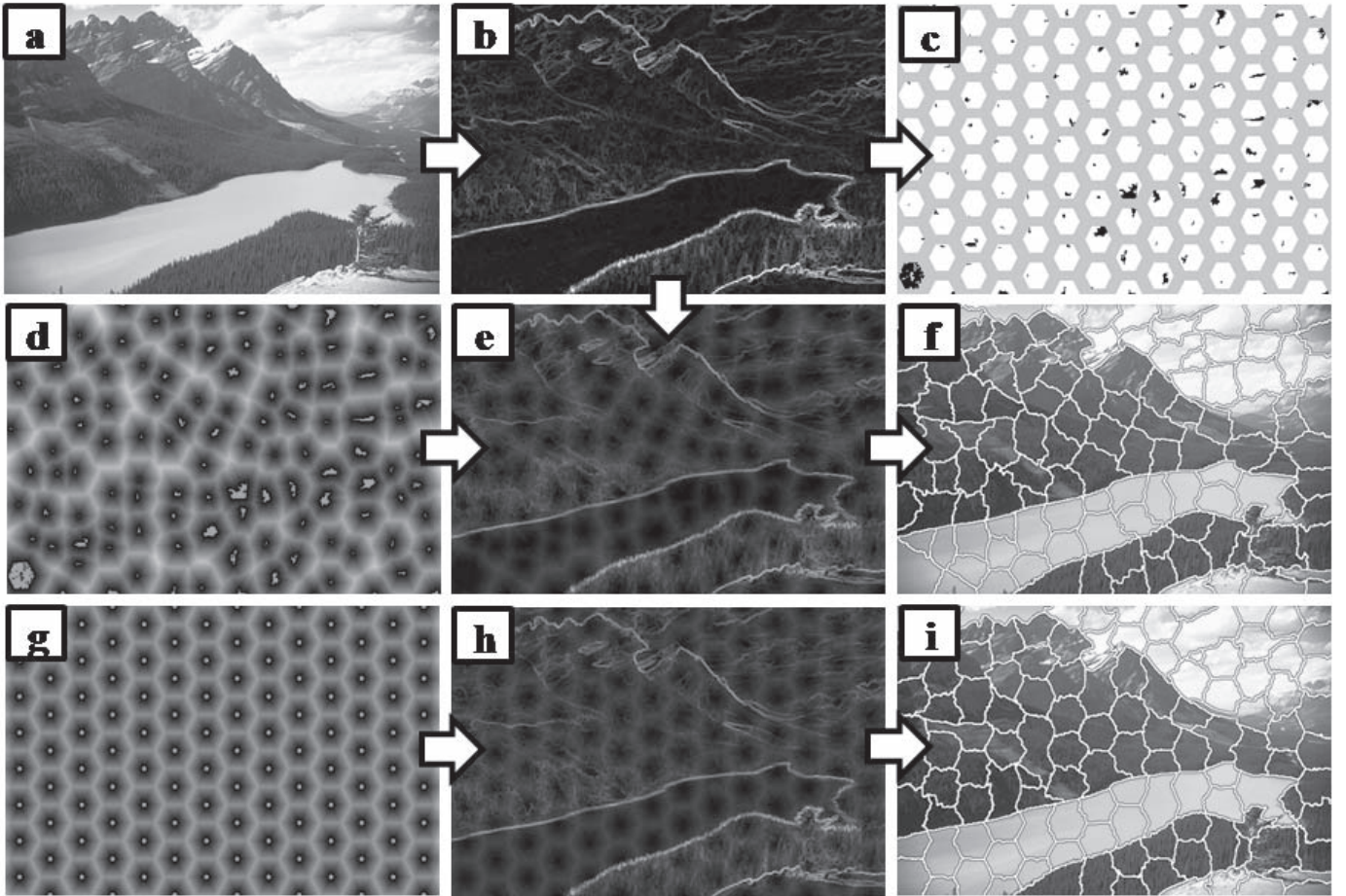


Fig. 2. Illustration of waterpixels generation: (a): original image; (b) corresponding Lab gradient; (c): selected markers within the regular grid of hexagonal cells (step $\sigma = 40$ pixels); (d): distance function to markers; (g): distance function to cell centers; (e) and (h): spatially regularized gradient respectively with distance functions to selected markers (d) and to cell centers (g); (f) and (i): Resulting waterpixels obtained by respectively applying the watershed transformation to (e) and (h), with markers (c).

271 have the same highest extinction value, or if more than one
 272 flat zone present the same lowest gradient value in the cell.
 273 Therefore, an additional step enables to keep only one of
 274 the connected components if there is more than one potential
 275 “best” candidate.

276 The set of resulting markers is denoted $\{M_i\}_{1 \leq i \leq N}$,
 277 $M_i \subset D$. The result of the marker selection procedure is
 278 illustrated in Figure 2.c.

279 C. Spatial Regularization of the Gradient and Watershed

280 The selection of markers has enforced the pertinence of
 281 future superpixel-boundaries but also the regularity of their
 282 pattern (by imposing only one marker per cell). In this
 283 paragraph, we design a spatially regularized gradient in
 284 order to further compromise between boundary adherence and
 285 regularity.

286 Let $Q = \{q_i\}_{1 \leq i \leq N}$ be a set of N connected components
 287 of the image f . For all $p \in D$, we can define a distance
 288 function d_Q with respect to Q as follows:

$$289 \quad \forall p \in D, d_Q(p) = \frac{2}{\sigma} \min_{i \in [1, N]} d(p, q_i) \quad (1)$$

290 where σ is the grid step defined in the previous section. The
 291 normalization by σ is introduced to make the regularization
 292 independent from the chosen SP size.

293 We have studied two possible choices of the q_i . The first one
 294 is to choose them equal to the markers: $q_i = M_i$. Resulting
 295 waterpixels are called m -waterpixels. The second one consists
 296 in setting them at the cell centers: $q_i = o_i$, which leads to
 297 c -waterpixels. We have found that the first gives the best
 298 adherence to object boundaries, while the second produces
 299 more regular superpixels.

300 The spatially regularized gradient g_{reg} is defined as follows:

$$301 \quad g_{reg} = g + kd_Q \quad (2)$$

302 where g is the gradient of the image f , d_Q is the distance
 303 function defined above and k is the spatial regularization
 304 parameter, which takes its values within \mathfrak{R}^+ . The choice of k is
 305 application dependent: when k equals zero, no regularization
 306 of the gradient is applied; when $k \rightarrow \infty$, we approach the
 307 Voronoi tessellation of the set $\{q_i\}_{1 \leq i \leq N}$ in the spatial domain.

308 In the final step, we apply the watershed transformation on
 309 the spatially regularized gradient g_{reg} , starting the flooding
 310 from the markers $\{M_i\}_{1 \leq i \leq N}$, so that an image partition
 311 $\{s_i\}_{1 \leq i \leq N}$ is obtained. The s_i are the resulting waterpixels.

IV. EXPERIMENTS

In order to evaluate waterpixels, the proposed method has been applied on the Berkeley segmentation database [20] and benchmarked against the state-of-the-art. This database is divided into three subsets, “train”, “test” and “val”, containing respectively 200, 200 and 100 images of sizes 321×481 or 481×321 pixels. Approximately 6 human-annotated ground-truth segmentations are given for each image. These ground-truth images correspond to manually drawn contours.

A. Implementation

We have found that it is beneficial to pre-process the images from the database using an area opening followed by an area closing, both of size $\sigma^2/16$ (where σ is the chosen step size of the regular grid). This operation efficiently removes details which are clearly smaller than the expected waterpixel area and which should therefore not give rise to a superpixel contour.

The Lab-gradient is adopted here in order to best reflect our visual perception of color differences and hence the pertinence of detected objects. The margin parameter ρ , described in III-A, is set to $\frac{2}{3}$.

The cell centers correspond to the vertices of a square or an hexagonal grid of step σ . The grid is computed in one pass over the image, by first calculating analytically the coordinates of the set of pixels belonging to each cell and then assigning to them the label of their corresponding cell. We will display the results for the hexagonal grid, as hexagons are more isotropic than squares. Interestingly, they also lead to a better quantitative performance, which was intuitively expected.

The implementation of the waterpixels was done using the Simple Morphological Image Library (SMIL) [21]. SMIL is a Mathematical Morphology library that aims to be fast, lightweight and portable. It brings most classical morphological operators re-designed in order to take advantage of recent computer features (SIMD, parallel processing, ...) to allow handling of very large images and real time processing.

B. Qualitative Analysis

Figure 3 shows various images from the Berkeley segmentation database and their corresponding waterpixels (m -waterpixels and c -waterpixels, hexagonal and square grids, different steps). Figures 3.b and 3.c (zooms of original image presented in 3.a for m -waterpixels and c -waterpixels respectively) show the influence of the regularization parameter k (0, 4, 8, 16) for an homogeneous (blue sky) and a textured (orange rock) regions. As expected, when $k \rightarrow \infty$, m -waterpixels tend towards the Voronoi tessellation of the markers, while c -waterpixels approach the regular grid of hexagonal cells. Both show good adherence to object boundaries, as shown in Figures 3.d, 3.e, 3.f. Of course, enforcing regularity decreases the adherence to object boundaries (see the zoom in Figure 3.f for $k = 16$). One advantage of waterpixels is that the user can choose the shape (and size) of resulting superpixels depending on the application requisites. Figure 3.d, for example, presents waterpixels for hexagonal (second and third columns) and square (fourth column) grids.

As a gradient-based approach, the quality of the watershed is dependant on the borders contrast. If we look at the contours

of objects missed by waterpixels, we see that it is due to the weakness of the gradient, as illustrated in Figure 4.

C. Evaluation Criteria

SP methods produce an image partition $\{s_i\}_{1 \leq i \leq N}$. In order to compute the SP borders, we use a morphological gradient with a 4 neighborhood. Note that the resulting contours are two pixels wide. To this set S_c , we add the one pixel wide image borders S_b . The final set is denoted C . The ground truth image corresponding to the contours of the objects to be segmented, provided in the Berkeley segmentation database, is called GT .

In superpixel generation, we look for an image decomposition into regular regions that adhere well to object boundaries. We propose to use three measures to evaluate this trade-off, namely boundary-recall, contour density and average mismatch factor, as well as computation time.

There are two levels of regularity: (1) the number of pixels required to describe the SP contours, which can be seen as a measure of complexity of individual SP, and (2) the similarity in size and shape between SP.

The first property is evaluated by the Contour Density, which is defined as the number of SP contour pixels divided by the total number of pixels in the image:

$$CD = \frac{\frac{1}{2}|S_c| + |S_b|}{|D|} \quad (3)$$

Note that $|S_c|$ is divided by 2 since contours are two-pixel-wide.

The second property, *i.e.* similarity in size and shape, is evaluated by an adapted version of the mismatch factor [22]. The mismatch factor measures the shape and size dissimilarity between two regions. Given two sets, A and B , the mismatch factor mf between them is defined as:

$$\begin{aligned} mf(A, B) &:= \frac{|A \cup B \setminus A \cap B|}{|A \cup B|} \\ &= 1 - \frac{|A \cap B|}{|A \cup B|} \end{aligned} \quad (4)$$

The mismatch factor and the Jaccard index thus sum to one. Aiming to measure the superpixel regularity, we adapted the mismatch factor to estimate the spread of size and shape distribution. Hence, the average mismatch factor MF is proposed as:

$$MF = \frac{1}{N} \sum_{i=1}^N mf(s_i^*, \hat{s}^*) \quad (5)$$

where s_i^* is the centered version of superpixel s_i , and \hat{s}^* is the average centered shape of all superpixels. The complete definition of the average mismatch factor is given in Appendix.

Note that although compactness is sometimes used in superpixels evaluation (see [23]), it is a poor measurement for region regularity. For example, perfectly-rectangular regions are regular but not compact (because they are different from discs). Waterpixels can in principle tend towards differently shaped superpixels (rectangles, hexagons or other), depending on the grid and the regularization function used. Since the average mismatch factor compares each superpixel against an

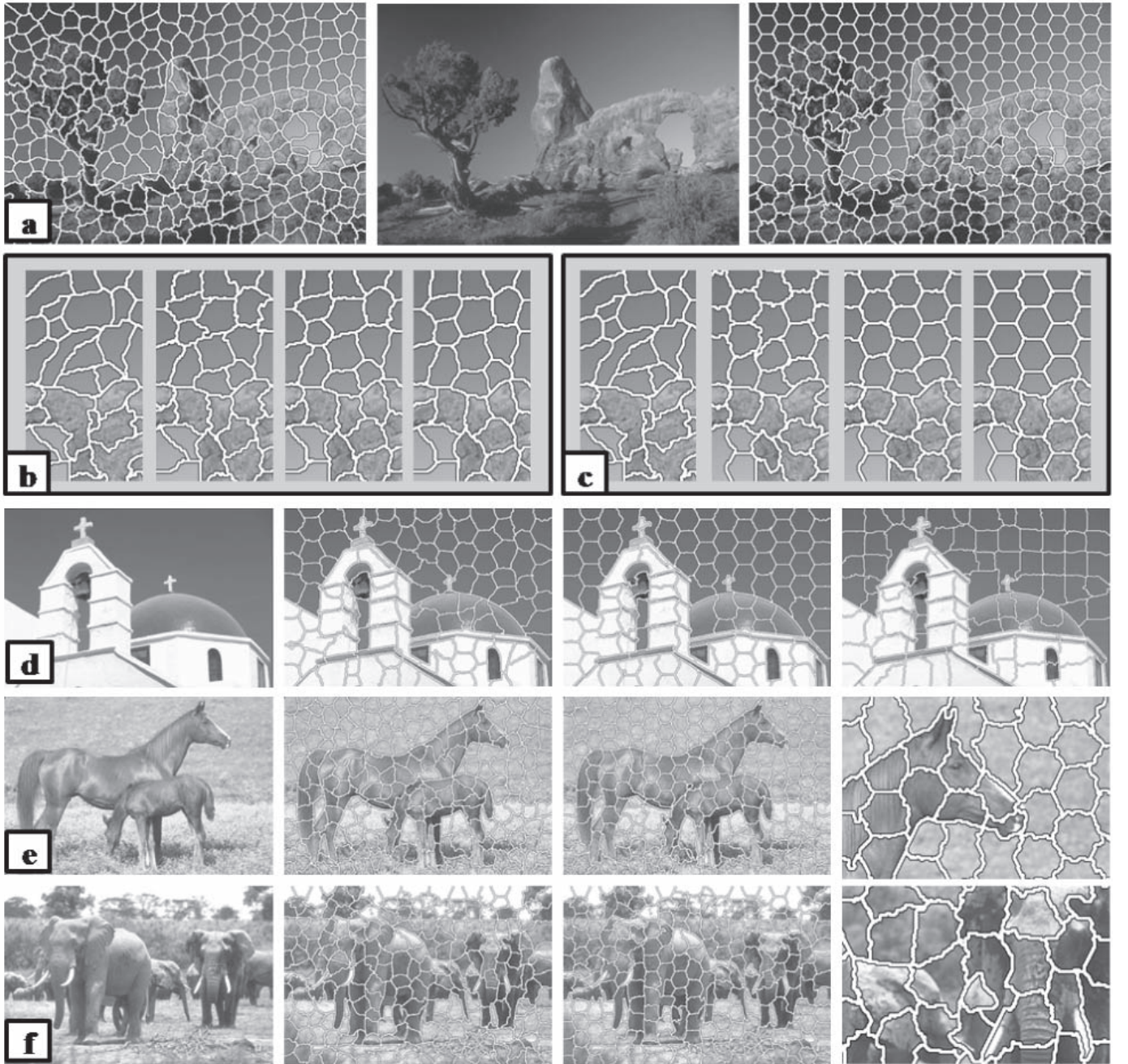


Fig. 3. Illustrations of waterpixels on the Berkeley segmentation database: All waterpixels images are computed with an hexagonal grid with step $\sigma = 30$ pixels and a regularization parameter $k = 8$, unless otherwise specified. (a): original image (middle) with corresponding *m-waterpixels* (left) and *c-waterpixels* (right). $\sigma = 25$ pixels, $k = 16$. (c): zooms of *m-waterpixels* (a) for $k = 0, 4, 8, 16$. (c): zooms of *c-waterpixels* (a) for $k = 0, 4, 8, 16$. (d): original image - *m-wat.* - *c-wat.* - *m-wat.* with square grid and $\sigma = 40$ pixels. (e): original image - *m-wat.* - *c-wat.* - zoom of *c-wat.*. (f): original image - *m-wat.* - *c-wat.* - zoom of *m-wat.* with $k = 16$.

418 image dependent template, this measure is more appropriate
419 to evaluate regularity than compactness.

420 To quantify the adherence to object boundaries, a classical
421 measure used in the literature is the boundary-recall (BR).
422 Boundary-recall is defined as the percentage of ground-truth
423 contour pixels GT which fall within strictly less than 3 pixels
424 from superpixel boundaries C :

$$425 \quad BR = \frac{|\{p \in GT, d(p, C) < 3\}|}{|GT|} \quad (6)$$

426 where d is the L_1 (or Manhattan) distance.

427 While precision cannot be directly used in the context of
428 over-segmentations, boundary-recall has to be, in this partic-
429 ular case of superpixels, interpreted with caution. Indeed, as
430 noted also by Kalinin and Sirota [24], very tortuous contours
431 systematically lead to better performances: because of their
432 higher number, SP contour pixels have a higher chance of
433 matching a true contour, increasing artificially the boundary-
434 recall. Hence, we propose to always consider the trade-off
435 between boundary-recall and contour density to properly
436 evaluate the adherence to object boundaries, penalizing at the
437 same time the cost in pixels to describe SP contours.

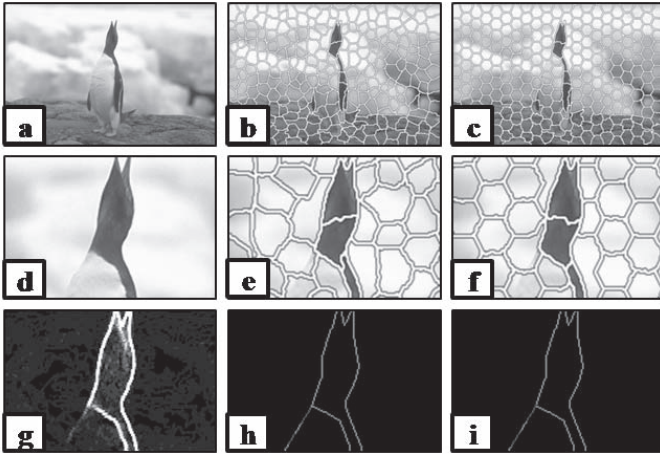


Fig. 4. Contours missed by waterpixels: (a): original image from the Berkeley segmentation database. (b): m -waterpixels with $step = 27$ and $k = 10$. (c): c -waterpixels with $step = 27$ and $k = 10$. (d), (e), (f): zoom of (a), (b), (c) respectively. (g): zoom of the non-regularized gradient image. (h) and (i): reached (green) and missed (red) contours, respectively by m -waterpixels and c -waterpixels.

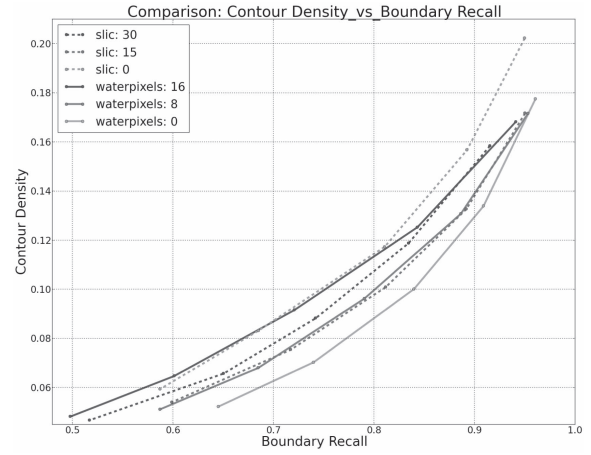
438 *D. Quantitative Analysis and Comparison*
 439 *With State-of-the-Art*

440 In this paragraph, we will use m -waterpixels and denote
 441 them directly as “waterpixels” for the sake of simplicity.

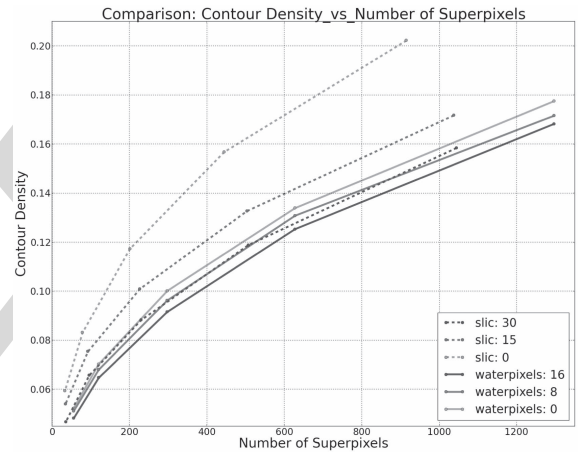
442 During the design of the algorithm, we used intermedi-
 443 ate results from the train and test subsets of the Berkeley
 444 database. Therefore, we report the results obtained for the
 445 validation subset (“val”), which contains 100 images. Results
 446 for boundary-recall, average mismatch factor and contour
 447 density are averaged for this subset and shown in Figure 5.
 448 Blue and red curves correspond to varying regularization
 449 parameters k and k' respectively for waterpixels and SLIC.
 450 The values for k and k' have been chosen such that they
 451 cover a reasonable portion of the regularization space between
 452 no regularization ($k = 0$) and a still acceptable level of
 453 regularization.

454 Figure 5(a) shows contour density against boundary-recall
 455 for waterpixels and SLIC. The ideal case being the lowest con-
 456 tour density for the highest boundary-recall, we can see that
 457 the trade-off between both properties improves for decreasing
 458 regularization, as expected. On the other hand, SLIC shows
 459 another behavior: the trade-off improves, then gets worse
 460 with regularization. At any rate, it is important to note that
 461 waterpixels achieves a better “best” trade-off than SLIC
 462 (see waterpixel $k = 0$ and SLIC $k' = 15$). Besides, this obser-
 463 vation is valid for the whole family of waterpixel-methods as
 464 the zero-value regularization does not take into account d_Q .
 465 In order to do a fair comparison between waterpixels and
 466 SLIC over all criteria, we choose corresponding curves in the
 467 trade-off contour density/boundary-recall, *i.e.* waterpixels with
 468 $k = 8$ and SLIC with $k' = 15$, and compare this couple for
 469 the other criteria.

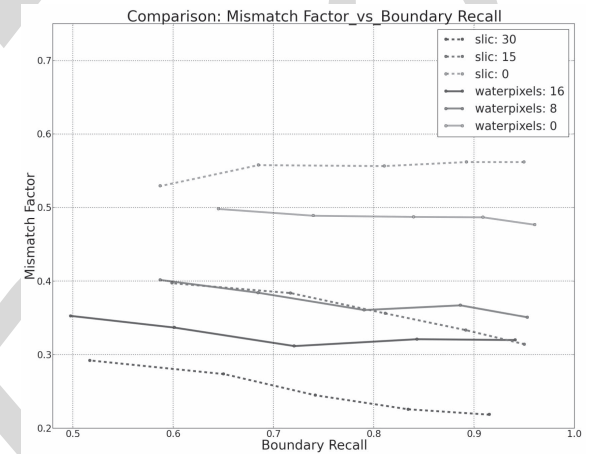
470 Figure 5(b) shows that, for a given number of superpixels,
 471 contour density of waterpixels is more stable and most of
 472 the time lower than SLIC when varying regularization. More
 473 particularly, contour density is lower for waterpixels ($k = 8$)



(a)



(b)



(c)

Fig. 5. Benchmark: performance comparison between waterpixels and SLIC. (a) Contour Density against Boundary-recall. (b) Contour Density against Number of Superpixels. (c) Mismatch factor against Boundary-recall.

474 than for SLIC ($k' = 15$). This means that for the same number
 475 of superpixels, waterpixels contours are shorter than SLIC
 476 contours, which is partly explained by less tortuous contours.

477 Figure 5(c) shows average mismatch factor against
 478 boundary-recall for waterpixels and SLIC. We can see that
 479 the curves for waterpixels with $k = 8$ and SLIC with $k' = 15$
 480 are here again close to each other. 480

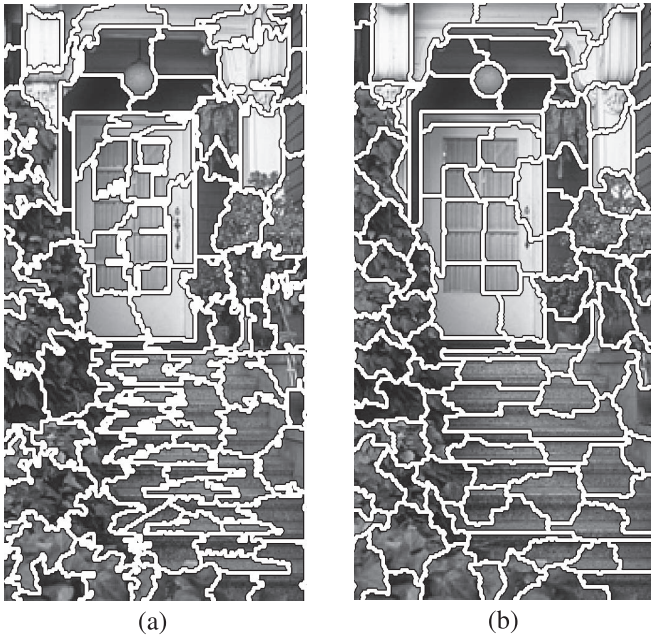


Fig. 6. Comparison between Waterpixels and SLIC superpixels for $\sigma = 25$ pixels on a zoom of an image from the Berkeley segmentation database. (a) SLIC $k' = 15$. (b) Waterpixels $k = 8$.

481 These properties are illustrated in Figure 6, where we can
 482 see examples of reached and missed contours by both methods,
 483 as well as their different behaviours in terms of regularity
 484 (shape, size, tortuosity).

485 E. Computation Time

486 Computing time was measured on a personal computer
 487 based on Intel(R) Core(TM) i7 central processing units
 488 (4 physical cores, 4 virtual ones), operating at 2.93GHz. Both
 489 methods have linear complexity with the number of pixels in
 490 the image. For an image of size 481×321 , average computing
 491 time for SLIC was 149 ms, and 132 ms for waterpixels
 492 (82 ms without pre-filtering). A more detailed comparison of
 493 computation times is presented in Figure 7 (showing average
 494 and standard deviation for different numbers of superpixels).
 495 We can see that waterpixels are generally faster to compute
 496 than SLIC superpixels. Contrary to the latter's, their compu-
 497 tation time decreases slightly with the number of superpixels.
 498 An analysis of computation times for the different steps of
 499 waterpixels reveals that this variability is only introduced by
 500 the grid computation and the minima selection procedure.
 501 Concerning grid computation time, it rises from 2 ms for
 502 small numbers of waterpixels to 27 ms for large numbers of
 503 waterpixels. This simply means that we still have to optimize
 504 this step. Concerning the computation time of the minima
 505 selection procedure, it decreases as waterpixels become larger
 506 because of pre-filtering step. Indeed, the size of this filtering
 507 is directly proportional to the cell size. As such, resulting
 508 images contain less minima, which simplifies the selection
 509 procedure. Besides, the variance observed when we change
 510 images is explained by the fact that the difficulty of minima
 511 evaluation/computation depends on the content of each image.

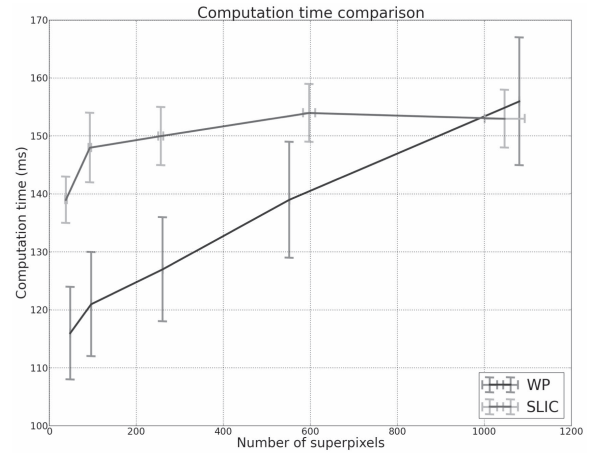


Fig. 7. Computation time comparison with images of the Berkeley database.

We are currently working on a new implementation of minima
 computation/evaluation which would be less dependent on the
 number of superpixels.

To conclude this section, waterpixels are generally faster
 to compute than SLIC superpixels, and they are at least
 as performant in the trade-off between adherence to object
 boundaries and regularity in shape and size, while using much
 less pixels to describe their contours.

V. DISCUSSION AND PERSPECTIVES

We have shown that waterpixels produce competitive results
 with respect to the state-of-the-art. These advantages are
 valuable in the classification/detection/segmentation pipeline,
 where superpixels play the part of primitives. Moreover, there
 is one major difference in the construction of the algorithm:
 the SLIC approach does not impose any connectivity con-
 straint. The resulting superpixels are therefore not necessarily
 connected, which requires some *ad hoc* postprocessing step.
 In contrast, waterpixels are connected by definition, and the
 connectivity constraint is actually implemented in the distance
 used.

The proposed approach is gradient-based. Standard methods
 can be used to compute this gradient, or a specific gradient
 computation method can be designed for a given application.
 In any case, this offers flexibility to waterpixels. One limitation
 though is the quality of the signal in such a gradient image.
 As seen in 4, alteration by noise or insufficiently contrasted
 contours may lead to the prevalence of regularity over adher-
 ence to object boundaries. If filtering steps are usually enough
 to deal with noise and remove non pertinent small details,
 parameter values have to be optimized for each database.
 Future work will aim at overcoming this limitation by adding a
 learning step of optimal filtering values for specific databases.

The general design of waterpixels offers many prospects.
 Among them, one promising field of improvement resides
 in the placement of markers, as they constitute the main
 degree of freedom of the method. We are currently investi-
 gating the possibility to select the markers in an optimal
 manner, for example by formulating the marker placement as a
 p -dispersion problem (see [25]) in an augmented space.

551 The speed of waterpixels contributes to expanding their
 552 possible applications. For example, it could be interest-
 553 ing to compute different sets of waterpixels, by changing
 554 design options (different cells, gradients, grid steps, etc.),
 555 and then use ensemble clustering methods to obtain a final
 556 segmentation [26], [27].

557 Last but not least, waterpixels lead to the efficient construc-
 558 tion of hierarchical partitions based on superpixels. Indeed,
 559 the computation of the watershed can produce at the same
 560 time a segmentation and a hierarchy of partitions based on
 561 that segmentation, with only minor overhead computation
 562 times [28]–[30].

563 VI. CONCLUSION

564 This paper introduces waterpixels, a family of methods
 565 for computing regular superpixels based on the watershed
 566 transformation. Both adherence to object boundaries and regu-
 567 larity of resulting regions are encouraged thanks to the choice
 568 of the markers and the gradient to be flooded. Different
 569 design options, such as the distance function used to spatially
 570 regularized the gradient, lead to different trade-offs between
 571 both properties. The computational complexity of waterpixels
 572 is linear. Our current implementation makes it one of the
 573 fastest superpixel methods. Experimental results show that
 574 waterpixels are competitive with respect to the state-of-the-art.
 575 They outperform SLIC superpixels, both in terms of quality
 576 and speed. The trade-off between speed and segmentation
 577 quality achieved by waterpixels, as well as their ability to
 578 generate hierarchical segmentations at negligible extra cost,
 579 offer interesting perspectives for this superpixels generation
 580 method.

581 An implementation of waterpixels is available from
 582 <http://cmm.ensmp.fr/~machairas/waterpixels>.

583 APPENDIX

584 MEAN MISMATCH FACTOR DEFINITION

585 Let $\{s_i\}_{1 \leq i \leq N}$ be a set of superpixels. The centered version
 586 s_i^* of s_i is obtained by translating s_i so that its barycenter is
 587 the origin of the coordinates system.

588 The average shape \widehat{s}^* of the $\{s_i\}$ is computed as follows.
 589 Let first define function S :

$$590 \quad S : \begin{cases} D & \longrightarrow \mathbb{N} \\ x_p & \longmapsto \sum_{i=1}^N 1_i(x_p) \end{cases} \quad (7)$$

591 where 1_i is the indicator function of s_i^* . Thus, image S cor-
 592 responds to the summation image of all centered superpixels.
 593 Let furthermore $\mu_A = 1/n \sum_{i=1}^N |s_i|$ be the average area of
 594 the considered superpixels, and let S_t be the threshold of S at
 595 level t : $S_t(x) = \{x_p \in D \mid |S(x_p)| \geq t\}$.

596 The average centered shape \widehat{s}^* is then the set S_{t_0} , where t_0
 597 is the maximal threshold value which enables \widehat{s}^* to have an
 598 area greater than or equal to μ_A :

$$599 \quad t_0 = \max\{t \mid |S_t| \geq \mu_A\} \quad (8)$$

$$600 \quad \widehat{s}^* = S_{t_0} \quad (9)$$

601 Finally, the mean mismatch factor of superpixels
 602 $\{s_i\}_{1 \leq i \leq N}$ is:

$$603 \quad MF = \frac{1}{N} \sum_{i=1}^N mf(s_i^*, \widehat{s}^*). \quad (10)$$

604 REFERENCES

- 605 [1] S. Beucher and C. Lantuéjoul, “Use of watersheds in contour detec-
 606 tion,” in *Proc. Int. Workshop Image Process., Real-Time Edge Motion*
 607 *Detection/Estimation*, 1979. AQ:5
- 608 [2] S. Beucher and F. Meyer, “The morphological approach to segmentation:
 609 The watershed transformation,” in *Mathematical Morphology in Image*
 610 *Processing*, E. Dougherty, Ed. 1993, pp. 433–481. AQ:6
- 611 [3] F. Meyer, “Un algorithme optimal pour la ligne de partage des
 612 eaux,” *Dans 8^e Congrès Reconnaissance Formes Intell. Artif.*, vol. 2,
 613 pp. 847–857, Nov. 1991.
- 614 [4] L. Vincent and P. Soille, “Watersheds in digital spaces: An efficient
 615 algorithm based on immersion simulations,” *IEEE Trans. Pattern Anal.*
 616 *Mach. Intell.*, vol. 13, no. 6, pp. 583–598, Jun. 1991.
- 617 [5] R. Achanta, A. Shaji, K. Smith, A. Lucchi, P. Fua, and S. Süsstrunk,
 618 “SLIC superpixels compared to state-of-the-art superpixel methods,”
 619 *IEEE Trans. Pattern Anal. Mach. Intell.*, vol. 34, no. 11, pp. 2274–2282,
 620 Nov. 2012.
- 621 [6] V. Machairas, E. Decencière, and T. Walter, “Waterpixels: Superpixels
 622 based on the watershed transformation,” in *Proc. IEEE Int. Conf. Image*
 623 *Process. (ICIP)*, Oct. 2014, pp. 4343–4347.
- 624 [7] X. Ren and J. Malik, “Learning an optimal region growing algorithm for image seg-
 625 mentation,” *Int. J. Pattern Recognit. Artif. Intell.*, vol. 1, nos. 3–4,
 626 pp. 351–375, 1987. [Online]. Available: <http://www.worldscientific.com/doi/abs/10.1142/S0218001487000242>
- 627 [8] B. Marcotegui and F. Meyer, “Bottom-up segmentation of image
 628 sequences for coding,” *Ann. Télécommun.*, vol. 52, nos. 7–8,
 629 pp. 397–407, 1997. [Online]. Available: <http://link.springer.com/article/10.1007/BF02998459>
- 630 [9] X. Ren and J. Malik, “Learning a classification model for segmentation,”
 631 in *Proc. 9th IEEE Int. Conf. Comput. Vis.*, vol. 1, Oct. 2003, pp. 10–17.
- 632 [10] P. F. Felzenszwalb and D. P. Huttenlocher, “Efficient graph-based
 633 image segmentation,” *Int. J. Comput. Vis.*, vol. 59, no. 2, pp. 167–181,
 634 Sep. 2004.
- 635 [11] A. Levinstein, A. Stere, K. N. Kutulakos, D. J. Fleet, S. J. Dickinson,
 636 and K. Siddiqi, “TurboPixels: Fast superpixels using geometric flows,”
 637 *IEEE Trans. Pattern Anal. Mach. Intell.*, vol. 31, no. 12, pp. 2290–2297,
 638 Dec. 2009.
- 639 [12] J. Wang and X. Wang, “VCells: Simple and efficient superpixels using
 640 edge-weighted centroidal Voronoi tessellations,” *IEEE Trans. Pattern*
 641 *Anal. Mach. Intell.*, vol. 34, no. 6, pp. 1241–1247, Jun. 2012.
- 642 [13] G. Zeng, P. Wang, J. Wang, R. Gan, and H. Zha, “Structure-sensitive
 643 superpixels via geodesic distance,” *Int. Conf. Comput. Vis.*, vol. 1, no. 1,
 644 pp. 1–27, 2011.
- 645 [14] O. Veksler, Y. Boykov, and P. Mehrani, “Superpixels and supervoxels in
 646 an energy optimization framework,” in *Proc. 11th Eur. Conf. Comput.*
 647 *Vis.*, 2010, pp. 211–224.
- 648 [15] P. Soille, *Morphological Image Analysis: Principles and Applications*.
 649 New York, NY, USA: Springer-Verlag, 2003.
- 650 [16] B. Andres, U. Köthe, M. Helmstaedter, W. Denk, and F. A. Hamprecht,
 651 “Segmentation of SBFSEM volume data of neural tissue by hier-
 652 archical classification,” in *Pattern Recognition*, Berlin, Germany:
 653 Springer-Verlag, 2008, pp. 142–152.
- 654 [17] J. Stawiński, E. Decencière, and F. Bidault, “Interactive liver tumor
 655 segmentation using graph cuts and watershed,” in *Proc. MICCAI*,
 656 New York, NY, USA, 2008.
- 657 [18] P. Neubert and P. Protzel, “Compact watershed and preemptive SLIC:
 658 On improving trade-offs of superpixel segmentation algorithms,” in
 659 *Proc. IEEE 22nd Int. Conf. Pattern Recognit. (ICPR)*, Aug. 2014,
 660 pp. 996–1001.
- 661 [19] C. Vachier and F. Meyer, “Extinction values: A new measurement
 662 of persistence,” in *Proc. IEEE Workshop Non Linear Signal/Image*
 663 *Process.*, 1995, pp. 254–257.
- 664 [20] D. Martin, C. Fowlkes, D. Tal, and J. Malik, “A database of human
 665 segmented natural images and its application to evaluating segmentation
 666 algorithms and measuring ecological statistics,” in *Proc. 8th IEEE Int.*
 667 *Conf. Comput. Vis.*, vol. 2, Jul. 2001, pp. 416–423.
- 668 [21] M. Faessel and M. Bilodeau, “SMIL: Simple morphological image
 669 library,” LRDE, Tech. Rep., 2013.
- 670 AQ:8

- 672 [22] N. J. C. Strachan, P. Nesvadba, and A. R. Allen, "Fish
673 species recognition by shape analysis of images," *Pattern*
674 *Recognit.*, vol. 23, no. 5, pp. 539–544, 1990. [Online]. Available:
675 <http://www.sciencedirect.com/science/article/pii/003132039090074U>
- 676 [23] A. Schick, M. Fischer, and R. Stiefelhagen, "An evaluation of the
677 compactness of superpixels," *Pattern Recognit. Lett.*, vol. 43, pp. 71–80,
678 Jul. 2014.
- 679 [24] P. Kalinin and A. Sirota, "A graph based approach to hierar-
680 chical image over-segmentation," *Comput. Vis. Image Understand.*,
681 vol. 130, pp. 80–86, Jan. 2015. [Online]. Available: <http://www.sciencedirect.com/science/article/pii/S1077314214001891>
- 682 [25] E. Erkut, "The discrete p -dispersion problem," *Eur. J. Oper. Res.*,
683 vol. 46, no. 1, pp. 48–60, May 1990.
- 684 [26] K. Cho and P. Meer, "Image segmentation from consensus informa-
685 tion," *Comput. Vis. Image Understand.*, vol. 68, no. 1, pp. 72–89,
686 Oct. 1997. [Online]. Available: <http://www.sciencedirect.com/science/article/pii/S1077314297905464>
- 687 [27] A. Strehl and J. Ghosh, "Cluster ensembles—A knowledge
688 reuse framework for combining multiple partitions," *J. Mach.*
689 *Learn. Res.*, vol. 3, pp. 583–617, Mar. 2003. [Online]. Available:
690 <http://dx.doi.org/10.1162/153244303321897735>
- 691 [28] F. Meyer, "Minimum spanning forests for morphological segmentation,"
692 in *Mathematical Morphology and Its Applications to Image Processing*.
693 Boston, MA, USA: Kluwer, Sep. 1994, pp. 77–84.
- 694 [29] S. Beucher, "Watershed, hierarchical segmentation and waterfall algo-
695 rithm," in *Mathematical Morphology and Its Applications to Image*
696 *Processing*, J. Serra and P. Soille, Eds. Fontainebleau, France: Kluwer,
697 Sep. 1994, pp. 69–76.
- 698 [30] F. Meyer, "An overview of morphological segmentation," *Int. J. Pattern*
699 *Recognit. Artif. Intell.*, vol. 15, no. 7, pp. 1089–1118, 2001.



702 **Vaia Machairas** received the Engineering degree in
703 optics from the Institut d'Optique Graduate School
704 (Supoptique), Palaiseau, France, and the master's
705 degree in optics, image, vision from Jean Monnet
706 University, Saint Etienne, France, both in 2013.
707 She is currently pursuing the Ph.D. degree with the
708 Centre for Mathematical Morphology, MINES Paris-
709 Tech. Her research interests include mathematical
710 morphology, image segmentation, machine learning,
711 and colorimetry.



712 **Matthieu Faessel** received the Ph.D. degree in
713 engineer sciences from the University of Bordeaux,
714 France, in 2003. He is currently a Research Engi-
715 neer with the Centre of Mathematical Morphology,
716 School of Mines, Paris, France. His research inter-
717 ests include image segmentation, computer vision,
718 and materials.



719 **David Cárdenas-Peña** received the bachelor's
720 degree in electronic engineering and the M.Eng.
721 degree in industrial automation from the Univer-
722 sidad Nacional de Colombia, Manizales-Colombia,
723 in 2008 and 2011, respectively. He is currently
724 pursuing the Ph.D. degree in automatics with the
725 Universidad Nacional de Colombia. He has been a
726 Research Assistant with the Signal Processing and
727 Recongnition Group since 2008. His current research
728 interests include machine learning and signal and
729 image processing.



730 **Théodore Chabardes** received the degree from the
731 Engineering School, ESIEE Paris, France, in 2014,
732 as an Engineer specialized in computer science.
733 He is currently pursuing the Ph.D. degree with
734 the Centre of Mathematical Morphology, School of
735 Mines, Paris, France. His research interests include
736 mathematical morphology, image segmentation, and
737 software optimization.



738 **Thomas Walter** received the Diploma degree in
739 electrical engineering from Saarland University,
740 Germany, and the Ph.D. degree in mathematical
741 morphology from Mines ParisTech, France. He held
742 a post-doctoral position with the European Molecu-
743 lar Biology Laboratory, Heidelberg, Germany. He is
744 currently a Team Leader in bioimage informatics
745 with the Centre for Computational Biology, Mines
746 ParisTech, and a member of the Bioinformatics Unit
747 with the Curie Institute, Paris. His most visible
748 scientific contributions have been in the field of
749 bioimage informatics, and in particular, in high content screening. He has
750 pioneered methods in the field of cellular phenotyping and phenotypic
751 clustering from live cell-imaging data. He was involved in the first genome-
752 wide screen by live cell imaging in a human cell line, and co-develops the
753 open-source software cellcognition.



754 **Etienne Decencière** received the Engineering degree
755 and the Ph.D. degree in mathematical morphology
756 from MINES ParisTech, France, in 1994 and 1997,
757 respectively, and the Habilitation à Diriger des
758 Recherches from Jean Monnet University, in 2008.
759 He holds a research fellow position with the Centre
760 for Mathematical Morphology, MINES ParisTech,
761 where he leads several academic and industrial
762 research projects. His main research interests are in
763 mathematical morphology, image segmentation, and
764 biomedical applications.

AUTHOR QUERIES

AQ:1 = Please check whether the edits made in the financial section are OK.

AQ:2 = Please confirm the current affiliation of all authors.

AQ:3 = Please confirm the postal code for “MINES ParisTech, PSL Research University, Center for Mathematical Morphology, Universidad Nacional de Colombia, Centre for Computational Biology, Institut Curie, and Inserm.”

AQ:4 = Table I is not cited in body text. Please indicate where it should be cited.

AQ:5 = Please provide the page range for ref. [1].

AQ:6 = Please provide the publisher name and location for ref. [2].

AQ:7 = Please provide the page range and also confirm the conference title for ref. [17].

AQ:8 = Please provide the organization, location, and report no. for ref. [21].

IEEE
Proof